Swimming and rafting of E.coli microcolonies at air-liquid interfaces

Giorgia Sinibaldi[a], Valerio Iebba[b], Mauro Chinappi[c,d]

[a]Department of Mechanical and Aerospace Engineering, Sapienza University of Rome, via Eudossiana 18, 00184, Rome, Italy
[b]Istituto Pasteur Cenci Bolognetti Foundation, Public Health and Infectious Diseases Dept., Sapienza University of Rome, P.le A. Moro 5, 00185, Rome, Italy
[c]Center for Life Nano Science, Istituto Italiano di Tecnologia, Viale Regina Elena 291, 00161, Rome, Italy,
[d]Department of Industrial Engineering, University of Rome Tor Vergata, Via del Politecnico, Rome 00133, Italy
e-mail:mauro.chinappi@uniroma2.it

Keywords: Microswimmers, Microcolony, *E.coli*

The dynamics of active colloidal suspension and swimming microorganisms is strongly affected by solid-liquid and air-liquid interfaces. In this contribution, the motion of *E.coli* at air-liquid boundary is analyzed. We observed and characterized the motion of both isolated *E.coli* and microcolonies. Both of them follow circular trajectories.
Single bacteria preferentially show a counter-clockwise motion. In few cases, complete circles are apparent (Fig 1B) while, the more frequent condition is characterized by circular arcs connected by cusps (Fig 1A). Each cusp corresponds to a tumbling phase where the *E.coli* momentarily stops its motion and changes swimming direction. CW and CCW motion of flagellated microswimmers close to an interface can be explained in terms of fluid dynamic interaction between the swimmer and the surface. No-slip boundary condition at the fluid interface gives rise to CW motion, while swimming close to a free-slip interface results in CCW trajectories [1-4]. CW swimmers are slightly slower than CCW ones, while no statistically significant difference is found concerning the radius of curvature R of the trajectories (p-value > 0.05), Fig 1C. The occurrence of a small percentage of CW swimming bacteria can be ascribed to the presence of molecules in the media that can alter the usual free-slip behavior of an air-liquid interface resulting in region with higher viscosity where no-slip or partial slip condition hold. Indeed, the local presence of high concentration of molecules secerned by the bacteria in specific regions, would result in an increase of the local viscosity [3]. This occurrence can explain also the smaller velocity of the CW swimmer.
Differently from the single swimmers, microcolonies do not show a preferential direction of rotation. CW (Fig 2D-F) and CCW (Fig 2A-C) rotations occur with the same probability (Fig 2G). The average speed of microcolonies is lower than single swimmer one and no significant difference in the speed of CW and CCW rotating colonies is observed. These occurrences indicate that the mechanism underlying the microcolony motion is different from the single swimmer. We propose a simple mechanical model where the microcolonies move like rafts constrained to the air-liquid interface to explain the experimental data.
Finally, we observed that the microcolony growth is due to the aggregation of colliding single-swimmers, suggesting that the microcolony formation resembles a condensation process where the first nucleus originates by the collision between two single-swimmers.

[1] Lauga, E., Di Luzio, W. R., Whitesides, G. M. & Stone, H. A. Swimming in circles: motion of bacteria near solid boundaries. Biophysical Journal 90, 400–412 (2006).
[2] Di Leonardo, R., Dell Arciprete, D., Angelani, L. & Iebba, V. Swimming with an image. Physical Review Letters 106, 038101 (2011).
[3] Lemelle, L., Palierne, J.-F., Chatre, E. & Place, C. Counterclockwise circular motion of bacteria swimming at the air-liquid interface. Journal of Bacteriology 192, 6307–6308 (2010).
[4] Pimponi, D., Chinappi, M., Gualtieri, P. & Casciola, C. Hydrodynamics of flagellated microswimmers near free-slip interfaces. Journal of Fluid Mechanics 789, 514–533 (2016).

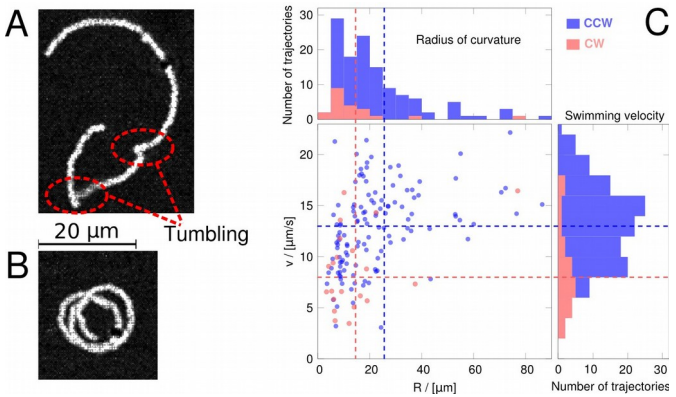

Figure 1. Single *E.coli*. The microswimmer trajectories are constituted by a sequence of circular arcs (A,B). The cusps between two consecutive arcs correspond to tumbling. C) Radius of curvature R *vs* swimming velocity *v*. Each point corresponds to a single circular arc. Red and blue points refer to CW and CCW trajectories, respectively. Horizontal and vertical dashed lines are the mean values. CCW swimmers move significantly faster than CW swimmers (p-value < 10 −6) while radius of curvature difference are not statistically significant (p-value > 0.05).

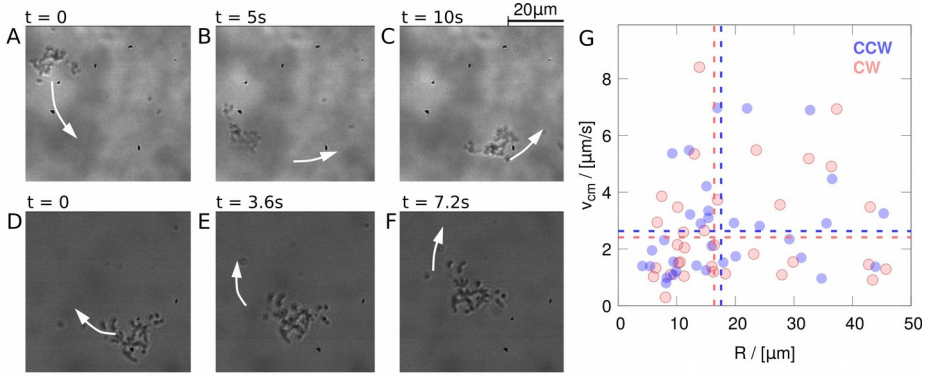

Figure 2. Microcolonies move like 2D rigid raft suspended at the air-liquid interface and exhibit both CCW (A-C) and CW motion (D-F). Panel G reports the scatter plot of the speed v_{cm} *vs* the radius of curvature *R* of the microcolony center. Red and blue symbols refer to CW and CCW motion of the raft center, respectively. CW motion occurs 52% of the cases while CCW 48%, the difference is not significant. Horizontal and vertical lines correspond to the average CW and CCW radius of curvature and speed. No significant difference is observed between CW and CCW for both average speed and radius of curvature.

Chaos and correlated avalanches in excitatory neural networks with synaptic plasticity

Fabrizio Pittorino,[1,2] Miguel Ibáñez-Berganza,[2] Matteo di Volo,[3] Alessandro Vezzani,[4,1] and Raffaella Burioni[1,2]

[1]*Dipartimento di Fisica e Scienza della Terra, Università di Parma, via G.P. Usberti, 7/A - 43124, Parma, Italy*

[2]*INFN, Gruppo Collegato di Parma, via G.P. Usberti, 7/A - 43124, Parma, Italy*

[3]*Group for Neural Theory, Laboratoire de Neurosciences Cognitives, INSERM U960, École Normale Supérieure, Paris, France*

[4]*IMEM-CNR, Parco Area delle Scienze, 37/A-43124 Parma, Italy*

e-mail: fabrizio.pittorino@gmail.com

Keywords: complexity, statistical physics, neuroscience

A collective chaotic phase with power law scaling of activity events is observed in a disordered mean field network of purely excitatory leaky integrate-and-fire neurons with short-term synaptic plasticity [1]. The dynamical phase diagram exhibits two transitions from quasi-synchronous and asynchronous regimes to the nontrivial, collective, bursty regime with avalanches. In the homogeneous case without disorder, the system synchronizes and the bursty behavior is reflected into a doubling-period transition to chaos for a two dimensional discrete map. Numerical simulations show that the bursty chaotic phase with avalanches exhibits a spontaneous emergence of persistent time correlations and enhanced Kolmogorov complexity. Our analysis reveals a mechanism for the generation of irregular avalanches that emerges from the combination of disorder and deterministic underlying chaotic dynamics.

---

[1] F. Pittorino, M. Ibáñez-Berganza, M. di Volo, A. Vezzani and R. Burioni, Phys. Rev. Lett. 118 (2017), 098102-6.

THE ROLE OF NEGATIVE LINKS IN BRAIN NETWORKS

Fabrizio Parente [a], Alfredo Colosimo [a]
[a] SAIMLAL Dept. , Sapienza University of Rome, Rome, Italy
e-mail: fabrizio.parente86@gmail.com

Keywords: Negative Links, Balance Theory, Brain Network, Network Theory, Multi Agent Systems

Functional connectivity studies focused more on positive than negative correlations, caused by the not well-defined nature of negative correlations. However, several authors pointed out the persistence of significant negative correlations and a possible physiological role for them [1-2-3]. A clear mechanism about how negative interactions are related to the positive one has not been proposed as yet and in such a context the Network Theory [4] is useful in providing general quantifiers of network topology and the Balance Theory helps in defining the conditions for the signed networks' functional stability [5]. Here we report about: 1) characterizing negative correlations in fMRI acquisitions of healthy people; 2) reproducing an equilibrium between different brain areas implementing a negative feedback mechanism in a Multi Agent System (MAS) for a small network model.

For the first issue, images from the 1000 Functional Connectomes Classic collection (180 healthy controls in resting state conditions, http://fcon 1000.projects.nitrc.org/indi/retro/BeijingEnhanced.html) was taken [6]. The images of each subject were divided into 90 Regions Of Interest (ROIs) and the correlation matrices were calculated (Figure 1)**.** Finally, a number of topological indexes were calculated for the positive and negative matrices separately: Efficiency (segregation-integration index), Assortativity and Rich-club coefficient [4]. The Assortativity calculates the probability of interaction among nodes in the entire network, while the Rich-Club coefficient [10] indicates the node interactions in a particular range of the node degree. Our results show that negative networks are characterized by a lower segregated structure as compared to positive networks, while the Assortativity assumed a negative value (nodes tend to be connected to other nodes with different node degree). The Rich-Club analysis demonstrates that this average trend of node degree interaction is kept only by the most connected nodes (Figure 2). The architecture emerging from our analysis describes a small number of central nodes less connected between each other but interacting with nodes of lower degree.

As for the second issue we describe a minimalistic computational model simulating the homeostatic regulation between regions having positive and negative correlations, and using the Balance Theory to define the conditions for the networks' functional stability [5]. The concept of balance refers to a triadic model in which agents can have positive or negative relation among them, thus the triangular graph is balanced (or stable) if cycling through it (by multiplying the links) produces a positive result (Figure 3). In this regard, a simple 9-node network representing a crude model of 9 interacting brain regions was made in a Multi Agents System (Figure 4), and reproduced in the NetLogo™ MAS programming environment (https://ccl.northwestern.edu/netlogo/): the scheme of a 9-node graph including three stable modules (A,B,C) connected among each other by negative connections. The stability in the scheme on the left can be reproduced, as testified by the finite value (= 2) of the <ShortestPathLength> (APL) if and only if the clockwise and anticlockwise direction of each links on the right model correspond to the positive and negative sign of the corresponding link on the left. Worthless to say that also the specular correspondence between sign and direction holds. By this strategy we obtained different activity levels among sub-networks by reversing the sign of some links or adding new links of reversed sign. We also represented the dynamics of the system by the energy flow through the links, up to the reaching of a stable state, as predicted by the Balance Theory.

In conclusion, we showed how a combined approach of experimental and MAS-based simulation techniques may clarify complex brain functions and, in principle, even explain some stability alterations of pathological significance.

[1] X. Chai et al., Neuroimage, 59(2012)1420-8.
[2] C. Chang and G. Glover, Neuroimage, 447 (2009) 1448-59.
[3] M. Fox et al., J Neurophysiol., 101 (2009) 3270-328.
[4] E. Bullmore and S. Bassett, Annu. Rev. Clin. Psychol., 7 (2011).
[5] F. Heider, Journal of Psychology, 21 (1946) 107-112.

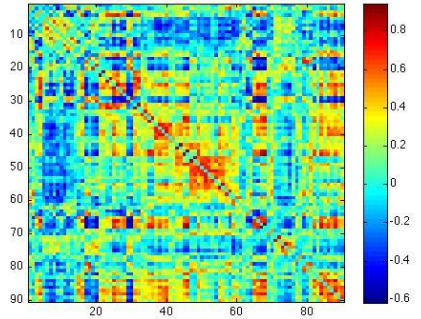

Figure 1. Correlation Matrix with positive and negative values between ROIs of a single subject from fMRI data. The raw data are plotted in a normalized, false color scale.

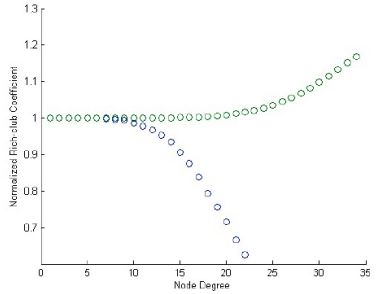

Figure 2. Rich-Club coefficient: blue dots negative networks, green dots positive networks. A node degree interval having a Rich-Club coefficient greater than 1 indicates a set of particular nodes more connected among each other; a Rich-Club coefficient lower that 1 refers to nodes avoiding reciprocal links.

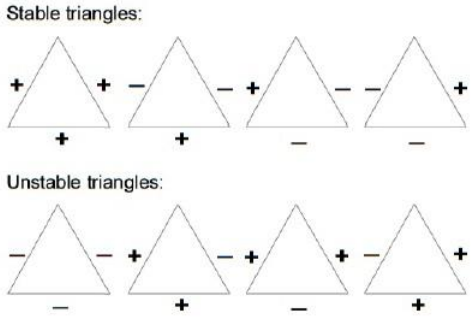

Figure 3. The sign multiplication of all stable configurations results in a positive value, and in a negative value for the unstable ones.

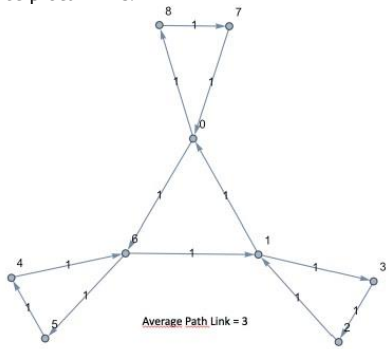

Figure 4. Simple 9-nodes network implemented in MAS. Notice the clockwise and anticlockwise direction of links within and between modules. The nodes are indicated by numbers (0 ... 8) and the links by weigths which, in the case of binary networks, = 1.

Whole Brain Mapping of the Hemodynamic Response Function

Mangini F[a,b], Moraschi M[a], Giove F[a,c]

[a]Centro Fermi, Museo Storico della Fisica e Centro Studi e Ricerche Enrico Fermi, Rome, 00184, Italy.
[b]Department of Information Engineering, Electronics and Telecommunications,
"La Sapienza" University of Rome, Rome, Italy
[c]Fondazione Santa Lucia IRCSS, Rome, 00142, Italy
e-mail: federico.giove@uniroma1.it

Keywords: (Hemodynamic Response Function, fMRI, BOLD, Human Connectome Project)

Functional Magnetic Resonance Imaging (fMRI) indirectly investigates neuronal activity from the associated vascular response. The observation of the Blood Oxygenation Level Dependent (BOLD) signal, which depends on local changes in deoxyhemoglobin concentration in the brain, allows to draw information on the underlying neuronal activity. Conventional approaches model BOLD response as the convolution of the HRF (hemodynamic response function, i.e. the response to an impulsive stimulation) and the known experimental conditions. Hence, accurate knowledge of the HRF is a fundamental issue in fMRI, preventing from false positive/negative results and both power and effectiveness loss [1].

Phenomenological models for the HRF spanned from a single canonical shape to the use of a basis set of more or less complex functions [1] and, to date, the investigation of the performance of these models is an ongoing challenge. Indeed, interpretation of BOLD response as neuronal activity changes is difficult for the complexity of the neurovascular coupling itself. Activity-related neural signal is task and region dependent and not constant over time [2]. The hemodynamic response reflects the integral across time of the neuronal/glial activity and saturates over time [3]. Moreover, statistical model of the HRF could be source of potential confounds leading to miss-modeling and incorrect inference [1].

Purpose of this study was to explore the shape of the HRF across tasks and brain regions in a large cohort of subjects, by means of the investigation of the distributions of parameters characterizing its magnitude, latency and duration.

Subjects (24 females and 24 males) included in this study were part of the Human Connectome Project (HCP) [4]. The stimulations, administered in blocked design, elicited several classes of neural processing, including visual, motion and somatosensory, emotional, language, relational, social and cognition. Stimulations and preprocessing are fully described elsewhere [5]. Functional analysis were performed on a voxel basis by modelling the signal as the convolution of the unknown HRF with task paradigm. We used two basis set for HRF: a combination of gamma function and its time and dispersion derivatives, and a combination of sine functions. The estimated HRF was then characterized by its parameters (FWHM and time-to-peak). In Figure1 and 2 the HRF time to peak and FWHM mapping of a representative subject were shown for two different neuronal processing (motion and cognitive), for gamma functions (a) and sine functions (b) combinations, in regions of statistically significant ($p<0.05$ FEW corrected) activation. Our results showed that HRF shape varies across activated regions and, although to a lesser extent, depending on set basis functions.

Changes across activates areas could be related to a different geometry of local vascular structures while differences across set basis functions could be expression of differences in model flexibility, estimate potential errors and different degree of freedom and power of collinear regressors, which depends on the number and type of set basis functions.

In agreement with [1], our results suggest that the choice of the HRF is fundamental to avoid model misspecification and to increase fMRI sensitivity. Moreover, characterizing HRF could be useful in the investigation of neurovascular coupling and its variation with aging and disease, since hemodynamic response is highly correlated to synaptic activity [2].

[1] Lindquist et al. Neuroimage. 2009 March; 45(1Suppl): S187–S198; [2] Logothetis NK. Neurosci. 2003; 23(10):3963–3971; [3] Friston KJ et al. Neuroimage. 2000; 12(4):466–477; [4] Van Essen et al. NeuroImage. 2013; 80:62-79; [5] Glasser et al. NeuroImage 80 (2016): 105-124

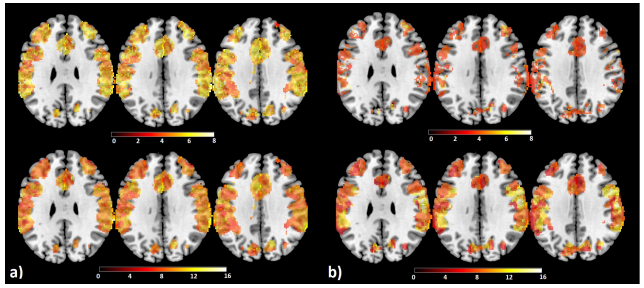

Figure1: Mapping of the HRF FWHM (up) and time-to-peak (bottom) of a representative subjects for the motion processing for (a) gamma functions and (b) sine functions combinations, in regions of statistically significant ($p<0.05$ FEW corrected) activation.

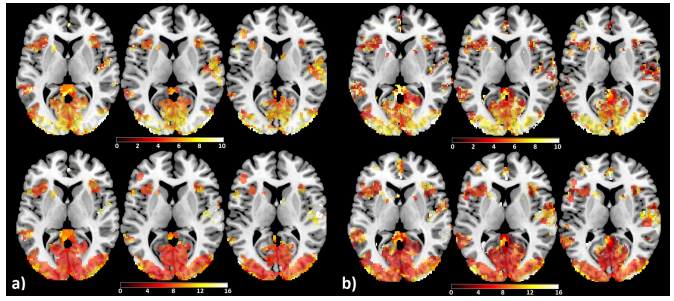

Figure2: Mapping of the HRF FWHM (up) and time-to-peak (bottom) of a representative subjects for the cognitive processing for (a) gamma functions and (b) sine functions combinations, in regions of statistically significant ($p<0.05$ FEW corrected) activation.

Unconventional DNA hydrogels as smart biomaterials

F. Bomboi [a], F. Romano [b], M. Leo [c], J. Fernandez-Castanon [d], R. Cerbino [e], T. Bellini [e], F.Bordi [a,d], P. Filetici [f] and F. Sciortino [a,d]

[a] ISC–CNR @ Sapienza Università di Roma, Roma, 00185, Italy
[b] Dip. di Scienze Molecolari e Nanosistemi, Università Ca' Foscari Venezia, Venezia Mestre, 30123, Italy
[c] Dipartimento di Biologia e Biotecnologie C. Darwin, Sapienza Università di Roma, Roma, 00185, Italy
[d] Dipartimento di Fisica, Sapienza Università di Roma, Roma, 00185, Italy
[e] Dipartimento di Biotecnologie Mediche e Medicina Traslazionale, Università degli Studi di Milano, Segrate (MI), Italy
[f] IBPM-CNR, Sapienza Università di Roma, Roma, Italy
e-mail: francesca.bomboi@gmail.com

Keywords: nanoscale biophysics, biocompatible hydrogels, smart biomaterials, DNA-nanotechnology

Thanks to its capability to hybridize in a programmable and reversible fashion, firstly exploited for nanotechnological purposes by N. Seeman [1], DNA has recently become a cornerstone in the development of innovative biomaterials, self-assembling designedly into complex meso/macroscopic structures of various shapes and functionalities. Within this field, a new promising road is opened by the use of DNA nanoconstructs as model systems to experimentally prove unconventional collective behaviours predicted in theoretical and numerical studies. DNA nanoconstructs offer indeed the outstanding chance of realizing bulk quantities of identical particles with tunable valence, selectivity and strength of interaction. Following this line, here we present the experimental realization of a new smart biomaterial: a biocompatible and thermo-reversible DNA-based hydrogel capable of melting both on heating and on cooling [2]. Such singular behaviour is indeed achieved by encoding competitive interactions in DNA sequences, thus programming both the shape of the resulting particles and their collective thermal behaviour.

Specifically, we experimentally reproduced the model of Ref. [3], which provides a theoretical archetype of a material that reversibly gels upon heating. In this model, composed by a binary mixture of tetravalent (A) and monovalent (B) patchy particles, the existence of two competing bonding patterns (i.e. entropically favoured AA bonds vs energetically favoured AB bonds) causes a peculiar re-entrant behaviour of the system, which undergoes, upon cooling, a continuous transition from fluid to gel to fluid again. Indeed, while at high temperatures the system behaves as a fluid of non-interacting A and B monomers, at low temperatures the relative strength of the AA/AB bonds defines the structure of the system: either a random tetrahedral network of A particles (i.e. a gel) or a fluid of AB_4 clusters (in which four B particles saturate all the patches of particle A). Additionally, at low densities, this system exhibits a re-entrant phase separation, giving rise to a Safran's like phase diagram [4], due to the competition between the two possible bondings.

In order to reproduce experimentally the predicted behaviour, we exploited DNA oligomers to produce high quantities of nanoconstructs with controlled valence and programmed interactions. Particularly, we used tetravalent DNA nanostars endowed with sticky-ends to provide interparticle bondings (previously tested as network-forming systems [5]), to mimic the A particles of the model and 6-base long single-stranded DNA sequences, specifically designed to compete with the AA bond at low temperatures, to reproduce the B ones. Fig. 1 shows a schematic of the AA and AB bonds as designed to experimentally realize the re-entrant gelation mechanism. With such choice, the system shows a peculiar temperature behaviour which is represented in Fig. 2. At high temperatures, nanostars spontaneously self-assemble by mixing four smartly-designed DNA strands (Fig. 2a-b). At intermediate temperatures (Fig. 2c), nanostars bind via sticky sequences forming a gel (B sequences have not yet hybridized). Eventually, at low enough temperatures (Fig. 2d), B competitors displace the AA bonds, creating freely diffusing AB_4 clusters.

Confirming the theoretical predictions, our results show that the system forms an highly viscous gel (signalled by an impressive slowing down of the dynamics monitored via dynamic light scattering) only in a restricted windows of temperatures centred around human body values and that the experimental phase diagram displays the expected re-entrant shape. The achievement of body-temperature gels able to dissolve at room temperature and interacting with biomolecules/antigens/drugs has the potential to act as an innovative delivery system to intensify bioactive substances in body tissues. We will thus present these biocompatible hydrogels, discussing how to create smart biomaterials with unconventional phase diagrams and tailor-made features by exploiting the versatility of DNA sequences.

[1] N. Seeman, Nature 421 (2003) 427– 430.
[2] F. Bomboi et al., Nat. Commun. 7 (2016).
[3] S. Roldàn-Vargas et al, Sci. Rep. 3 (2013) 2451.
[4] T. Tlusty and S. A. Safran, Science 290 (2000) 1328–1331.
[5] S. Biffi et al, PNAS 110 (2013) 15633–15637.

.

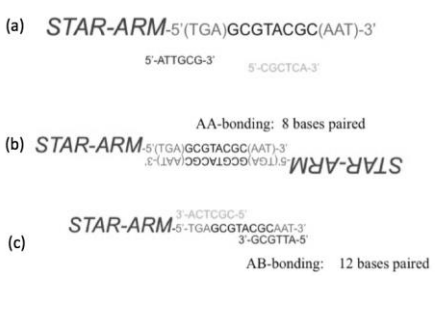

Figure 1. DNA sequences and scheme of the interactions. (a) Sequences composing the sticky terminals of the nanostar-arms and 6-base long sequences acting as competitors. (b) Sequence arrangement in presence of an AA bond (the bond leads to the formation of 8 base pairs) (c) Sequence arrangement in presence of an AB bond (the bond leads to the formation of 12 base pairs).

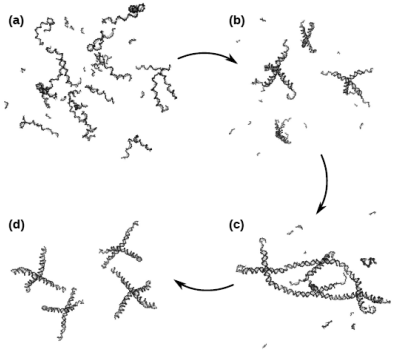

Figure 2. Temperature behaviour of the re-entrant gel. (a) Very high temperatures: the nanostar-forming sequences and the competitors are all not hybridized. (b) High temperatures: nanostars are formed while the competitors have not yet hybridized. (c) Intermediate temperatures: nanostars bind via the sticky ends forming a gel. (d) Low temperatures: competitors displace the AA bonds (diffusive AB_4 structures).

Gold coated silicon nanowires for near-infrared thermal treatment of cancer cells and in-situ Raman monitoring of the process evolution

Annalisa Convertino[a], Valentina Mussi[b], Luca Maiolo[a], Mario Ledda[c], Maria Grazia Lolli[c], Massimiliano Rocchia[d], Antonella Lisi[c]
[a] Institute for Microelectronics and Microsystems-CNR, Rome, 00133, Italy
[b] Institute for Complex Systems-CNR, Rome, 00133, Italy
[c] Institute Translational Pharmacology-CNR, Rome, 00133, Italy
[d] Thermo Fisher Scientific, Rodano (MI), 20090, Italy
e-mail: annalisa.convertino@cnr.it

Keywords: (nanowires, NIR photothermal treatment, cancer cells, Raman spectroscopy)

The use of nanotechnology in cancer therapy promises the development of novel approaches or the improvement of the existing ones with minimal invasive treatments able to eliminate selectively the cancer cells without damaging the healthy tissues. In this perspective, photothermal therapy (PTT) assisted by nanomaterials has recently emerged as a very promising strategy to overcome the intrinsic limitations of the conventional surgery because of unique advantages including high specificity, minimal invasiveness and precise spatio-temporal selectivity [1, 2].
In this work we report on the capacity of highly disordered and randomly oriented gold covered silicon nanowire (Au/Si NW) array to induce the photothermal death of cancer cells and monitor in situ the evolution of the treatment. We fabricated 2-3 μm long SiNWs by Plasma Enhanced Chemical Vapor Deposition (PECVD) and covered with an evaporated Au layer, 150 nm thick. A monolayer of human colon adenocarcinoma cells (CaCo-2), a popular cancer in vitro model [3] commonly employed for biopharmaceutical evaluations, was directly grown to confluence onto the Au/SiNWs and then irradiated by infrared laser at 780 nm. We found the laser irradiation to efficiently induce the death of several tens of CaCo-2 cells within a localized area and allow simultaneously the recording of Raman spectra from the irradiated zone following the evolution of the treated cells.
Furthermore the proposed material is also characterized by very attractive features such as *i.* the enhanced NIR absorption in a large range overlapping the I, II, and III biological windows; *ii.* the ease and scalable fabrication methodology compatible with polymeric or glasses supports which provide an effective method to integrate the Au/Si NWs in optical fiber laser devices [4,5]; the cell friendly behavior. These remarkable properties make the Au/SiNWs suitable to be integrated in optical fiber laser devices for endoscopic therapies with intraoperative monitoring and as platform to develop novel photothermal treatments by using different cancer cell lines and NIR laser source

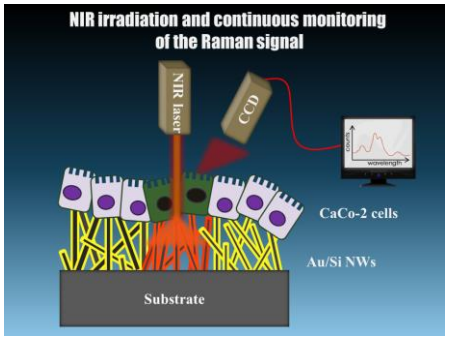

Figure 1.Schematic representation showing NIR irradiation of a monolayer of CaCo-2 cells grown on Au/SiNWs and continuous Raman signal monitoring.

[1] L. Cheng, C. Wang, L. Feng, K. Yang, Z. Liu, Chem. Rev. 114 (2014) 10869–10939.
[2] N. S. Abadeer and C. J. Murphy, J. Phys. Chem. C 120 (2016) 4691–4716.
[3] V. Meunier et al, Cell Biol. Toxicol. 11 (1995) 187-194.
[4] L. Maiolo, D Polese, A Pecora, G Fortunato, Y Shacham-Diamand, A. Convertino. Adv. Healthcare Mater. 5 (2016) 575–583.
[5] A. Convertino, V. Mussi, L. Maiolo, Sci Rep. 2016; 6: 25099
.

On the interaction of carbon nanotubes and microalgae

Taras K. Antal[a], Alena A. Volgusheva[a], Silvia Orlanducci[b,c], Gianluca Fulgenzi[d], Andrea Margonelli[c], Teresa Lavecchia[c], Giuseppina Rea[c], Maya D. Lambreva[c]

[a] Department of Biophysics, Faculty of Biology, Lomonosov Moscow State University, 119992 Moscow, Russian Federation
[b] Department of Chemical Science and Technology, University of Rome Tor Vergata, 00133 Rome, Italy
[c] Institute of Crystallography, National Research Council of Italy, 00015 Monterotondo Scalo, RM, Italy
[d] Department of Molecular and Clinical Sciences, Marche Polytechnic University, 60126 Ancona, Italy

e-mail: maya.lambreva@mlib.ic.cnr.it

Keywords: carbon nanotubes, nanomaterials, biotechnology, microalgae, photosynthesis

A critical mass of knowledge is emerging on the interactions between plant cells and engineered nanomaterials, revealing the potential of plant nanobiotechnology to promote and support novel solutions for the development of a competitive bioeconomy. Application of carbon nanotubes (CNTs) in plant biotechnology and agriculture brought to light an increasing amount of new findings, revealing the potential of CNTs to promote plant growth and crop production, or to control the delivery of fertilizers or pesticides to crops [1,2]. Furthermore, the combination of highly dynamic and adaptive plant cell structures with easily manipulated inorganic material at nanoscale level paved the way for a new emerging technology, the so called plant nanobionics, which promised not only to improve plant photosynthetic features but also to impart plants with new and enhanced functions [3,4]. The plant nanobionics approach suggested the capability of CNTs to increase the efficiency of solar energy harnessing in the photosynthetic process and improve cell response to oxidative stress conditions [3]. This new knowledge may foster the exploitation of the nanotechnology tools to empower photosynthetic performance and production yields of commercially important microalgal species.

Large-scale cultivation of microalgae in photo-bioreactors plays an important role in the production of biomass, biofuels or high-value compounds [5]. One of the main problems in high-density-cultured algal bioreactors is the reduction of production yield due to occurrence of strong light-shading. Besides, very often, the introduction of different stress conditions (e.g. nutrients starvation) is exploited to redirect the algal metabolism towards the synthesis of desired compounds. Thus, experimental strategies taking advantages of SWCNT ability to assist the photosynthetic electron transport and the cell uptake of engineered nanoparticles or molecules with antioxidant or signaling functions bare great capacity to improve fitness and photosynthetic performance of commercially important photosynthetic microorganisms under large-scale manufacture conditions [6]. Here we will discuss the potential of the CNTs to enhance functions of algae facilitating a more efficient use of photosynthetic algal systems in the sustainable production of valuable goods. The research is focused on the development of experimental approaches to enable the interactions of photosynthetic microorganisms and CNTs, and to study the effects of CNT properties on algal fitness and photosynthetic performance, and nanotubes uptake into algal cell.

[1] P. Wang et al., Trends Plant Sci. 21 (2016) 699-712.
[2] S. Guatimosim et al., In: *Bioengineering Applications of Carbon Nanostructures*, A. Jorio (ed.), Springer International Publishing Switzerland 2016, pp. 17-29.
[3] J.B. Giraldo et al., Nature Mater. 13 (2014) 400-408.
[4] M.H. Wong et al., Nature Mater. 16 (2017) 264-272.
[5] Ooms et al. 2016 Nature Comms. 7 (2016) 12699.
[6] M.D. Lambreva et al., Photosynth. Res. 125 (2015) 451-471.

High-sensitivity screening of soluble ERBB2 in different cell lines using a combined label-free and fluorescence biosensing platform

A. Sinibaldi[a], M. Allegretti[b], N. Danz[c], P. Munzert[c], E. Sepe[a], C. Sampaoli[d], A. Occhicone[a], E. Tremante[b], P. Giacomini[b], and F. Michelotti[a]

[a] SAPIENZA University of Rome, Rome, 00161, Italy
[b] Regina Elena National Cancer Institute , Rome, 00144, Italy
[c] Fraunhofer Institute for Applied Optics and Precision Engineering IOF, Jena, 07745, Germany
[d] IRCCS Ospedale Pediatrico Bambino Gesù, Rome, 00146, Italy
e-mail: alberto.sinibaldi@uniroma1.it

Keywords: Optical biosensors, Bloch surface waves, 1D photonic crystals, ERBB2, Breast cancer

ERBB2 (also known as Neu, or HER2) is a tyrosine kinase receptor that acts as master integrator of epidermal growth factor receptor signaling, and regulates a variety of cell proliferation, growth and differentiation pathways. In particular, ERBB2 overexpression occurs in approximately 20–30% of breast cancers and unless treated with ERBB2-targeted therapies this breast cancer subtype is associated with a dismal prognosis, collocating breast cancer as the most common, potentially fatal cancer of women [1].
According to international guidelines (College of American Pathologist, http://www.cap.org), the target therapy based on Trastuzumab is administered when IHC staining either reaches a 3+ intensity, or is at least 2+ and the gene is amplified, as assessed by FISH. This method, although accurate and highly standardized, relies on semi-quantitative, subjective IHC scores, and yields a discontinuous scale. In the present work, we propose a new analytical technique that is able to quantify very low concentrations of ERBB2 cancer biomarkers in biological complex matrices.
In particular, we report on the use of one-dimensional photonic crystal (1DPC) biochips to detect clinically relevant concentrations of ERBB2 expressed in different cell lines. To do that, we have developed an optical platform, combining both label-free and fluorescence detection, which makes use of 1DPC biochips tailored with monoclonal antibodies for highly specific biological recognition. The excitation of a Bloch surface wave (BSW) is obtained by a prism coupling system leading to a dip in the angular reflectance spectrum [2]. Similar to surface plasmon resonance, the measurement of the shift of the position of such a dip, due to refractive index perturbations at the surface, is exploited for biosensing (Label-free mode, LF). Moreover, in the presence of fluorescent labels at the surface, the platform analyses the BSW biochip also in the enhanced fluorescence mode, thus obtaining further information on the cancer biomarker assay and making bio-recognition more robust and sensitive [3]. For fluorescence operation mode (FLUO), a limit of detection below 1 ng/mL, about 10 times lower than label-free approach, has been attained, enabling an ultimate resolution for ERBB2 quantitation that is used to successfully discriminate cell lines over-expressing different amounts of ERBB2. Such a method definitely meets international recommendations (15 ng/mL) for diagnostic ERBB2 assays that in the future may help to more precisely assign therapies counteracting cancer cell proliferation and metastatic spread. Further development of the platform, leading to the fabrication of an integrated point-of-care instrument making use of plastic disposable biochips [4], will be also reported.

[1] S. Dawood et al., 2010, J. Clin. Oncol. 28 (1), 92–98.
[2] A. Sinibaldi et al., Sensors and Actuators B, 2012, 174, 292.
[3] A. Sinibaldi et al., Biosensors & Bioelectronics, 2017, 92, 125–130.
[4] N. Danz et al., Proc. SPIE, 2015, 9506, 95060V;

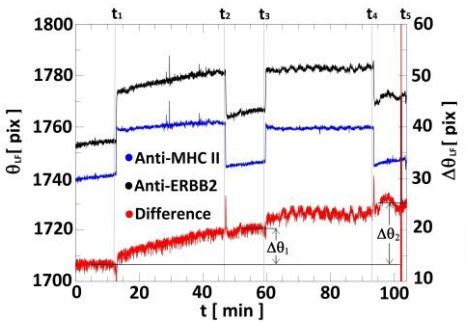

Figure 1. Label-free sensograms recorded during the calibration procedure for the detection of ERBB2 spiked in D-PBS 1X at 20 ng/mL. The curves are for the signal spot (black, left axis), reference spot (blue, left axis) and difference (red, right axis).

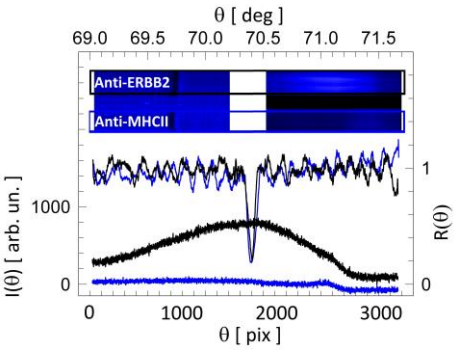

Figure 2. Experimental curves recorded by the CCD camera during the assay with ERBB2 spiked in D-PBS 1X. The curves refer to either LF (top curves) or FLUO (bottom curves) operation for the signal (black) and reference (blue) sensing spots. R(θ) (right axis) shows the BSW resonance in the LF mode. I(θ) shows DyLight 650 fluorescence emission. (Insets) CCD images in the LF (left) and FLUO (right) modes. In both images the top region is the signal spot and the bottom region is the reference spot.

Conducting polymers and composite hydrophilic biopolymers: new approaches to produce biomimetic systems

Rocco Carcione[(a)], Melania Reggente[(c)], Teresa Lavecchia[(a)], Mariglen Angjellari[(a,b)], Maria Letizia Terranova[(a,b)], Marco Rossi[(b,c)], Emanuela Tamburri[(a,b)]

[(a)] Dipartimento di Scienze & Tecnologie Chimiche , Università di Roma "Tor Vergata", 00133 Roma, Italy

[(b)] Nanoshare s.r.l.,00131, Rome, Italy

[(c)] Dipartimento di Scienze di Base e Applicate per l'Ingegneria, Sapienza Università di Roma, 00161 Roma, Italy

e-mail: emanuela.tamburri@uniroma2.it

Keywords: (nanocomposites, bio-interfaces, bio-electrodes)

The need to produce new biomaterials for a wide range of applications, including artificial muscles, neural interfaces and biosensors, is driving the attention of the scientific community towards the class of conductive polymers (CP) and of hydrophilic biopolymers.
As regards the CPs, due to their intrinsic conductivity, the good charge-transfer properties and the low impedance, they can be used as coating of implantable electro-stimulation electrodes providing interfaces suitable to improve soft-tissue integration [1].
Moreover the volume changes induced by the charge-compensating ions flowing into or from their backbone during oxidation/reduction processes, make CP promising electrochemomechanical systems to be explored for production of artificial muscles [2,3].
We present here the realization of innovative bio-electrodes , based on Titanium sheets coated with conductive and boron free diamond films onto which thin layers of different CP (polyaniline, polypirrole, polythiophene) have been subsequently electrodeposited.
Structural and morphological features as a function of process time, applied potential or current flow through the sample have been investigated performing cyclic voltammetry experiments simultaneously to topographic imaging by means of electrochemical atomic force microscopy technique. The conformational movements produced by the re-organization of double bonds along the chains during CP redox reactions have been monitored and are proposed as possible new artificial motor systems [4].
In the scenario of new materials, also the development of nanocomposites based on hydrophilic biopolymers and nanostructured carbons is considered a compelling task. In our labs nanocomposite layers made by PVA and oxidized graphene (GO) platelets have been prepared by an innovative procedure in which the in situ cross-linking of vinyl alcohol with maleic anhydride is carried out in the presence of the carbon filler [5].
The composite eco-friendly and biodegradable material shows enhanced mechanical and electrical properties with respect to pure PVA . The high processability , the facility of casting and of film forming , coupled with the high flexibility and the totally reversible stretchability under dry conditions and in the swollen state , make the PVA/GO nanocomposites promising bio-mimetic model materials .

[1] M.R. Abidian and D.C. Martin, Biomaterials, 29(9) (2008) 1273-1283.
[2] T.F. Otero and J.G. Martinez, J. Mater. Chem. B (2013) 1-26.
[3] M.J. Higgins, S.T. McGovern and G.G. Wallace, Languimir 25(6) (2009) 3627-3633.
[4] E. Tamburri et al. In: 15th IEEE International Conference on Nanotechnology - IEEE-NANO 2015, art. n. 7388782, pp. 979-982,
[5] T. Lavecchia et al., AIP CONFERENCE PROCEEDINGS (2016) Vol. 1736, No. 1, p. 02005.

Behaviour of multi-responsive soft microgels

Valentina Nigro [1,2], Roberta Angelini[2,1] and Barbara Ruzicka[2,1]

[1]Dipartimento di Fisica, Sapienza Università di Roma, Roma, 00185, Italy
[2]Istituto dei Sistemi Complessi del Consiglio Nazionale delle Ricerche (ISC-CNR), UOS Sapienza, Roma, 00185, Italy

e-mail: valentina.nigro@uniroma1.it

Keywords: (colloids, responsive microgels, polymers)

Responsive microgels are very attractive soft colloidal systems with high sensitivity to external stimuli, such as temperature, pH, electric field, ionic strength, solvent, external stress or light. This novel class of smart materials has attracted great interest in the last years, since their effective volume fraction and their elastic properties can be changed by tuning their response to the environmental conditions. This high versatility allows to modulate the interparticle potential and their reversible Volume-Phase Transition (VPT) (swelling/shrinking behaviour), making them suitable candidates for possible medical applications, such as controlled drug delivery, design of biomaterials, tissue engineering or as carriers for metallic nanoparticles [1].

Their typical behaviour may be even more complex and exotic by using two homopolymeric networks with independent responsiveness to different external stimuli. In particular by interpenetrating a thermo-sensitive polymer, the poly (N-isopropylacrylamide) (PNIPAM), and a pH-sensitive polymer, the poly (acrylic acid) (PAAc), we have obtained an Interpenetrated Polymer Network (IPN) microgel, sensitive to both temperature and pH. In this way we are able to tune the delicate balance between polymer/polymer and polymer/solvent interactions by changing pH or by varying the PAAc concentration. This allows to directly control the microgel softness and to explore how the elastic properties affect the dynamic arrest and the phase behaviour.

We propose a novel phase diagram for PNIPAM-PAAc IPN microgels, obtained by combining different experimental techniques. A swollen-shrunken volume phase transition at low concentrations and an ergodic to non-ergodic transition at the highest investigated concentrations, strongly dependent on pH and PAAc content, have been observed through Dynamic Light Scattering (DLS) [2] and Differential Scanning Calorimetry (DSC). The microgel local structure [3] and the exact nature of the observed non-ergodic state (gel and/or glass) have been investigated through Small-Angle Neutron Scattering (SANS) and Small-Angle X-Ray Scattering (SAXS) respectively. Moreover a comparison with numerical simulation, as previously done for other colloidal systems [4,5], will provides more insight on the interparticle interaction potential.

[1] Z. Dai and T. Ngai, J. Polym. Sci., Part A: Polym. Chem. 51 (2013) 2995-3003.
[2] V. Nigro, R. Angelini, M. Bertoldo, V. Castelvetro, G. Ruocco, and B. Ruzicka. J. Non-Cryst. Solids 407 (2015) 361-366.
[3] V. Nigro, R. Angelini, M. Bertoldo, F. Bruni, M.A. Ricci, and B. Ruzicka. J. Chem. Phys. 143 (2015) 114904.
[4] B. Ruzicka, E. Zaccarelli, L. Zulian, R. Angelini, M. Sztucki, A. Moussaïd, T. Narayanan, and F. Sciortino. Nat. Mater. 10 (2011) 56-60.
[5] R. Angelini, E. Zaccarelli, F.A. de Melo Marques, M. Sztucki, A. Fluerasu, G. Ruocco and B. Ruzicka. Nat. Commun. 5 (2014) 4049.

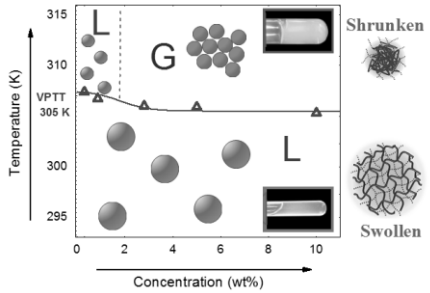

Figure 1. Phase diagram for colloidal suspensions of PNIPAM-PAAc IPN microgels in the investigated temperature and concentration range.

Sensitivity to heavy-metal ions of cage-opening fullerene quantum dots

E. Ciotta[1], P. Prosposito[1], P. Tagliatesta[2], C. Lorecchio[2], I. Venditti[3], I. Fratoddi[3], R. Pizzoferrato[1]

1. Department of Industrial Engineering, University of Rome-Tor Vergata, Rome, 0133, Italy

2. Department of Chemical Science and Technology, University of Rome-Tor Vergata, Rome, 0133, Italy

3. Department of Chemistry, University of Rome Sapienza, Rome, I-00185, Italy

e-mail: pizzoferrato@uniroma2.it

Keyword: (chemical sensors, heavy metals, graphene, quantum dots, GOQDs)

Heavy metals are potentially toxic elements and are highly related to the environment and humans health. The heavy metal streams that are traced in nature have undergone a sharp increase due to the anthropic activity of the last century, at times reaching critical levels of toxicity for flora, fauna and people [1].

Heavy metals tend to accumulate in the environment because they are not destroyed by normal biological and chemical cycles. The progressive increase of the pollutants in the environment is the major problem originating from bioaccumulation.

These metals can be absorbed by living organisms through the respiratory tract, by ingestion of food or water. Pb, Cd, Cu, Zn, Ni, Co, As, Bi, Sb, and Hg have a high tendency to form stable organometallic complexes with the phosphoryl groups of phospholipids rich in nerve cells and cause mutations in the DNA that can cause the onset of tumors.

To monitor these metals, it is necessary to develop efficient sensors which can be pursued also by using nanomaterials and nanostructures.

Recent studies [2] have demonstrated that the photoluminescence (PL) of aqueous solution of GOQDs, prepared by a variety of different methods, can be selectively quenched in presence of some heavy-metal ions (Hg^{2+}, Fe^{2+}, Cu^{2+}, Pb^{2+}). This characteristic has attracted the interest of researchers in view of implementing fast and cheap sensors for those heavy metals that are long known to be harmful to environment and toxic for human health. However, few experimental studies have been carried so far and they reported quite scattered and partially contradictory results which seem to depend on the synthesis method and the experimental conditions. Very recently, an innovative approach to preparation of photoluminescent carbon nanosheets was developed by Pumera *et al.* by using the low-temperature cage-opening of C_{60} buckminsterfullerene [3]. Due to the buckminsterfullerene structure, this material is like graphene oxide quantum dots (GOQDs) but with a different lattice structure, in fact, the carbon Cage-Opening Quantum Dots (COQDs) have a lattice made of both hexagons and pentagons. This could give rise to a different configuration of sp^2 domains, defects and functional groups which, in turn, could produce a new scenario for the response to chemical environment.

In this study, we have carried out a systematic evaluation and characterization of the quenching effect produced by some commonly encountered metal ions (Co^{2+}, Cu^{2+}, Ni^{2+}, Pb^{2+}, Cd^{2+}, As^{3+}) on the PL of COQDs prepared with a modified Hummers method. Typical absorption and fluorescence spectra assured the successful synthesis of COQDs, while the average size of nanoparticles was found to be 4 nm as measured by Dynamic Light Scattering (DLS). Figure 1 shows the quenching of the photoluminescence spectra with different concentrations of Cu^{2+}. As evident, the PL intensity gradually decreases with the increase of Cu^{2+} concentrations. The up-ward Stern-Volmer plot (not shown) indicates a combination of static quenching (complexation) and dynamic quenching. Similar curves, with a lower dependence on the ion concentration, were recorded for Pb^{2+} and As^{3+}, while substantially no response was found to Ni^{2+}, Co^{2+} and Cd^{2+}, as reported in Figure 2 which illustrates the inverse of the PL quenching in the presence of different ions at a concentration of 100 μM. Interestingly, the absorption spectrum is significantly modified only in presence of $Cu^{2+}$and Pb^{2+}, with the disappearance of the π-π* peak, while in the case of As^{3+} the curve shows much smaller variations. Moreover, only in the case of Pb^{2+} an evident brownish precipitate was observed at the bottom of the titration cuvette, which suggests a greater level of complexation leading to aggregation of COQDs. We believe these differences are quite important since they allow a selective detection of each of the three specific ions.

[1] Alloway, Brian J. Springer Netherlands, (2013) 3-9.
[2] J. Ju, and W. Chen. Current Organic Chemistry, (2015) 19 (12), 1150-1162.
[3] C. K. Chua, Z. Sofer, P. Simek, O. Jankovský, K. Klímová, S. Bakardjieva, et al. Acs Nano (2015) 9 (3), 2548-2555.

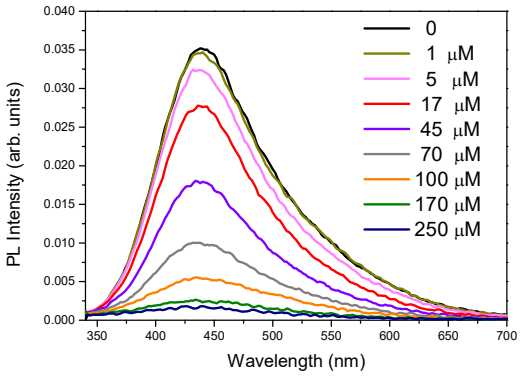

Figure 1. Fluorescence emission spectra of COQDs with different concentrations of Cu^{2+}. The PL intensity decreases with the increase of ions concentration.

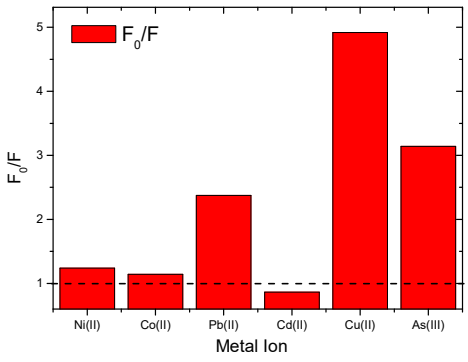

Figure 2. Sensitivity of COQDs to the different ions at a concentration of 100 μM

Multivariable reentrant condensation of microgel-polyelectrolyte complexes

Simona Sennato [a], Domenico Truzzolillo [b], Chiara Bazzoni [c], Stefano Sarti [c], Federico Bordi [a,c]

[a] Institute for Complex Systems (ISC), CNR, 00185 Rome, Italy
[b] Laboratoire Charles Coulomb (L2C), CNRS-Université de Montpellier, F-34095 Montpellier, France
[c] Physics Dept. La Sapienza University 00185 Rome, Italy

e-mail: simona.sennato@roma1.infn.it

Keywords: smart microgel, PNIPAM, controlled aggregation, volume phase transition

Recently, “smart" or “environmentally-sensitive” polymeric microgels have rapidly gained importance in materials science owing to their versatile applications, ranging from drug delivery to sensing and fabrication of advanced materials for photonics [1].
These nm- or micron-sized hydrogel particles are able to respond to external stimuli such as temperature, pH, or ionic strength by undergoing a rapid transition, at a critical value, from a swollen hydrophilic state to a collapsed hydrophobic state (volume phase transition, VPT). Depending on the external conditions, their behaviour falls between that of hard-sphere and ultra-soft colloids, making them very attractive in soft matter science, and giving rise to applications in several fields. The most widely studied material of this kind is based on the polymer poly(N-isopropylacrylamide) (pNIPAM) [1]. It can be cross-linked during synthesis to obtain microgel particles with a VPT of approximately 33 °C in water.
Indeed, the amount of applicative work on microgels is overwhelming with respect to attempts to grasp the fundamental understanding of the physical mechanisms behind the functional properties of multiresponsive microgels. In particular, it is well known that electrostatic interactions play a crucial role in the colloidal stabilization and phase behavior of charged microgel systems, as well as in the control of the uptake of small charged drugs to use microgel as stimuli-responsive drug delivery vectors. To fully control these processes understanding the electrostatics of microgels is essential.
Despite of that only a few investigations focus attention on electrostatic aspects [2].
Within this panorama, we investigated the multivariable controlled aggregation of pNIPAM microgels in the presence of the ε-polylysine, a small biocompatible polycation by means of Dynamic and Dielectrophoretic Light Scattering, Dielectric Spectroscopy and TEM Microscopy. We showed that increasing temperature above the VPT, polycation adsorption is promoted by the accumulating negative charge of collapsed microgel, giving rise to charge inversion and overcharging phenomena, accompanied by the formation of stable clusters with size and charge controlled by polycation/microgel molar ratio at the isoelectrical point. This peculiar electrostatically-driven controlled aggregation, known as reentrant condensation and deeply investigated in other class of soft colloids [3], is here primarily tuned by the VPT-transition of pNIPAM and opens new intriguing scenarios for the controlled self-assembly of soft colloids.

[1] R. Pelton, Temperature-sensitive aqueous microgels, Advances in Colloid and Interface Science 85 (2000) 1-33
[2] M. Quesada-Pérez and A. Martín-Molina, Monte Carlo simulation of thermo-responsive charged nanogels in salt-free solutions, Soft Matter 9 (2013)7086-7094
[3] S. Sennato et al. Salt-induced reentrant stability of polyion-decorated particles with tunable surface charge density, Colloids and Surfaces B: Biointerfaces 137 (2016) 109-120.
.

Study of colloidal suspensions of multi-responsive microgels

B. P. Rosi[a], V. Nigro[a,b], R. Angelini[a,b], B. Ruzicka[a,b],

[a] Dipartimento di Fisica, Sapienza Università di Roma, P.le Aldo Moro 5, 00185 Roma, Italy.
[b] Istituto dei Sistemi Complessi del Consiglio Nazionale delle Ricerche (ISC-CNR), sede Sapienza, Pz.le Aldo Moro 5, I-00185 Roma, Italy

e-mail: benedetta.rosi@gmail.com

Keywords: soft matter, microgel, IPN structure, phase diagram, drug delivery

Research on colloidal systems has attracted great interest in the last years, due to the variety of their technological applications and for the investigation of physical fundamental problems. Among these, suspensions of soft colloids have an even more complex and interesting behaviour with respect to hard ones. In particular, multi-responsive soft microgels, particles of typical size in the range 1 nm ÷ 1 μm, are characterized by the swelling behaviour, the ability to absorb and release a large amount of solvent in response to temperature variations (figure 1). The system undergoes a volume phase transition (VPT) from a swollen, hydrated phase to a shrunken, dehydrated one. This property strongly characterizes the microgel and leads to its application in many fields, such as pharmaceutical (drug delivery [1]), biomedical and bio-engineering (bioactive paper [2]). Microgel suspensions are also very important for the study of the glass transition, their softness gives rise to a variety of behaviours with respect to hard colloids [3]. In this study we focus on Interpenetrated Polymer Network (IPN) microgels of PNIPAM (thermo-responsive polymer) and PAAc (pH-responsive polymer) [4,5] two homopolymeric networks that respond independently to temperature and pH. Dynamical properties have been investigated through Dynamic Light Scattering (DLS) and the relaxation time, related to the hydrodynamic radius of the particle, has been measured. The relaxation time of PNIPAM microgels as a function of temperature shows a sharp discontinuity at the volume phase transition temperature (VPTT) since the particles expel the solvent and decrease drastically in size. IPN microgels at increasing PAAc content show a progressive reduction of the volume phase transition amplitude (figure 1). Moreover the relaxation time increases after the VPTT for increasing microgel concentration, diverging more significantly for high PAAc content (figure 2). Structural properties have been investigated through Small Angle X-Ray Scattering (SAXS) performed at the European synchrotron radiation facility ESRF. At low PAAc content and high concentrations, IPN microgels exhibit a crystal-to-liquid transition in correspondence of the VPTT (as found in pure PNIPAM microgels). At high PAAc content they show a crystal-to-liquid transition at low concentrations and a liquid-to-glass transition at high concentrations. With this study a first experimental phase diagram for IPN microgels has been drawn (figure 3).

[1] S. V. Vinogradov, Curr. Pharm. Des., 12:4703-4712, 2006.
[2] S. Su, Md Monsur Ali, C.D.M. Filipe, Y. Li, R. Pelton, Biomacromolecules 9:935–9419, 2008.
[3] J. Mattsson, H. M. Wyss, A. Fernandez-Nieves, et al., Nature 462:83-86, 2009.
[4] V. Nigro, R. Angelini, M. Bertoldo, et al., Journal of Non-Crystalline Solids 407:361-366, 2015.
[5] X. Xia and Z. Hu., Langmuir, 20:2094-2098, 2004.

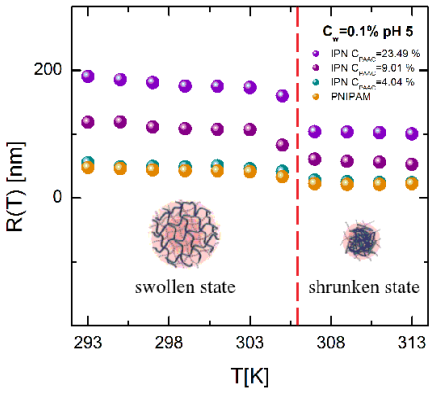

Figure 1. Hydrodynamic radius, as a function of the temperature, of PNIPAM and IPN PNIPAM/PAAc microgels.

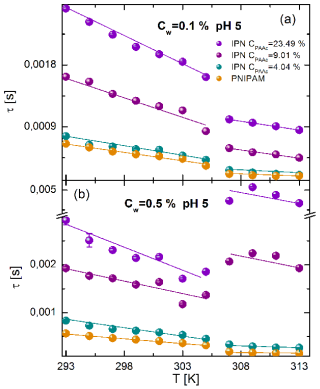

Figure 2. Relaxation time as a function of the temperature under varying PAAc content at low (a) and high (b) microgel concentration.

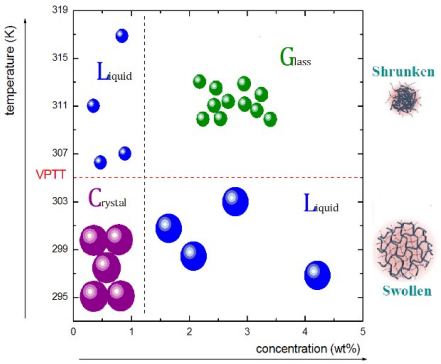

Figure 3. Phase diagram of IPN microgels at high PAAc content.

Investigation of gel behavior in FmocF-F_n polipeptides

M. Daniele,[a d] S. Sennato,[b] L.Chronopoulou,[c] F. Domenici[a], C. Palocci[c], S. Lupi[a], F. Bordi[a]

[a] *Physics Dept. La Sapienza University of Rome, Rome, Italy*
[b] *CNR-ISC Istitute for Complex Systems, Rome, Italy*
[c] *Chemistry Dept. La Sapienza University of Rome, Rome, Italy*
[d] *Physics Dept. University of study of L'Aquila, L'Aquila, Italy*

e-mail: mdaniele@lnf.infn.it

Keywords: Hydrogel, Dynamic Light Scattering , Fourier Transform Infrared Spectroscopy

Hydrogel constitute a group of polymeric materials, whose hydrophilic structure renders them capable of holding large amounts of water in their three-dimensional networks. The development of hydrogels capable of supporting the growth and proliferation of cells for tissue engineering applications is a rapidly expanding field of study [1], [2]. Some hydrogels are able to respond to stimuli of their surrounding environments. Examples of these stimuli include light, temperature, pH, and the electrical field.

A biocompatible gels such as Fluorenylmethyloxycarbonyl-L-phenylalanine (FmocF) is used for biomedical application. Unfortunately, the gelation mechanism in these systems remains poorly understood, thus strongly limiting their potential application. We explored two different gelation routes, a combined change in Temperature and concentration.

We studied the gel formation and structure by Dynamic Light Scattering (DLS), Fourier Transform Infrared Microscopy (FTIR) and Scanning Electron Microscope (SEM).

[1] A. Keller, A. Kolliod, Polymere 231 (1969) 386.
[2] B.Lotz, H. D. J Keith, Molec. Biol. 1971, 61. 201 .

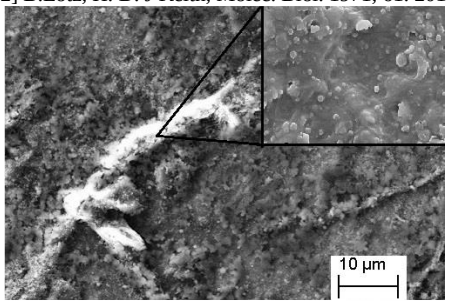

Figure 1. SEM Imaging of FmocF-FF. In the inset, zoom of sample on nanofiber.

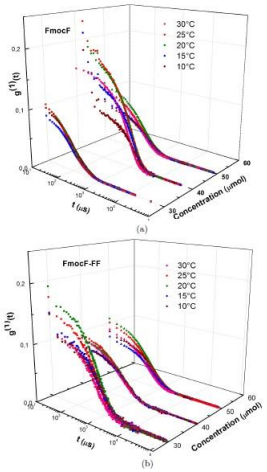

Figure 2. 3-Dimensional plot of g(1) vs concentration and correlation time at different temperatures near the gel transition for the FmocF (a) and FmocF-FF (b) systems.

Peptide aggregation in 2D: the relevance of peptide secondary structure and dynamics

Mariano Venanzi, [a] Mario Caruso, [a] Emanuela Gatto,[a] Ernesto Placidi,[b] Marta De Zotti, [c]
Fernando Formaggio,[c] Claudio Toniolo [c]
[a] Dept. of Chemical Sciences and Technologies and [b] Dept. of Physics, University of Rome Tor Vergata, Rome, 00133, Italy
[c] Institute of Biomolecular Chemistry, Padova Unit, CNR, University of Padova, Department of Chemistry, Padova, 35131, Italy
e-mail: venanzi@uniroma2.it

Keywords: peptide aggregation, Langmuir-Blodgett film, Atomic Force Microscopy.fibrillization

Very recently, we showed that a single-residue substitution inhibits fibrillization of an Ala-based pentapeptide, functionalized at the N-terminus with a pyrenyl (Py) group.[1] Aggregation was induced by adding water to micromolar methanol solutions of the two pentapeptides investigated, differing by the insertion of an helicogenic α-aminoisobutyric acid (Aib) replacing an Ala residue at position 4 (Figure 1). Aggregation was essentially driven by the hydrophobic effect, however, it was demonstrated that the secondary structure attained by the two peptides finely tunes the morphology of the peptide aggregates at the nano- and meso-scales, as shown by atomic force microscopy imaging.[1]
In this contribution, we report on the formation of Langmuir-Blodgett films of the same two pentapeptides.

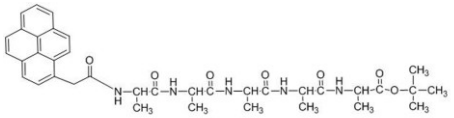

Py-CH_2-CO-(L-Ala)$_5$-OtBu (PyA5)

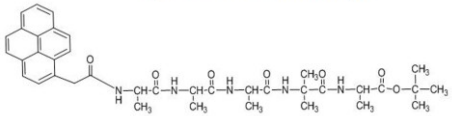

Py-CH_2-CO-(L-Ala)$_3$-Aib- L-Ala -OtBu (PyA3UA)

Figure 1. Amino acid sequences and acronyms of the two peptides investigated.

It will be shown that, also in the case of aggregation driven by surface pressure, the peptide secondary structure perturbation induced by the Aib substitution deeply affects the phase transition leading to the formation of the peptide film, together with its morphology and 2D organization.
In particular, surface pressure (π) vs. molecular mean area (Mma) isotherms indicate that while for **PyA5** the film formation can be considered a quasi-reversible process, a remarkable hysteresis was observed in the case of **PyA3UA,** suggesting irreversible changes caused by the compression of the peptide film, most likely due to the formation of 3D aggregates.
Interestingly, the emission spectrum of **PyA5** on quartz is dominated by excimer emission, the characteristic emission of an ordered array of Py*-Py excited state complexes. On the contrary, the spectrum of **PyA3UA** is typical of the pyrene monomer emission, with only a minor contribution from excimer species.

The results of AFM measurements carried out on the **PyA5** LB monolayer are reported in Figure 2(left). Figures 2A and 2B show micrometric globular structures connected by peptide nanometric filaments, while in the Figures 2C and 2D (left) a densely packed array of peptide fibers is imaged.
It should be noted that the packing of the peptide fibers occurs with a remarkable orientational order, as a result of both attractive interactions between the peptide fibers and the compression exerted by the mobile barriers.
AFM imaging of **PyA3UA** LB monolayers strengthen these considerations. In this case, only micrometric globular structures could be obtained on the hydrophilic mica surface, as shown by the images reported on the right of Figure 2.

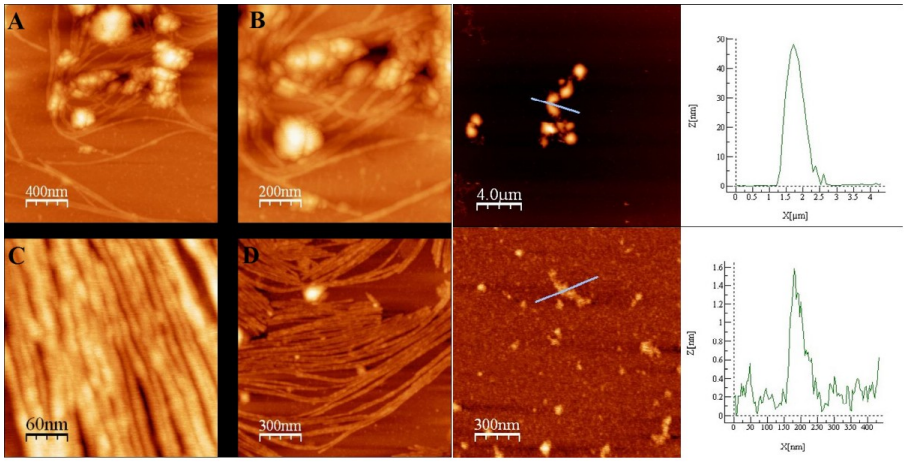

Figure 2 AFM images of Langmuir-Blodgett film of **PyA5** (left) and **PyA3UA** (right) on a mica substrate. On the far right, the height profile taken along the light-blue lines drawn on the right images are reported.

These findings indicate that the perturbation of the peptide conformational structure and dynamics induced by the Aib vs. Ala substitution, strongly affects the hierarchical self-assembly of the peptide building blocks, not only in solution, but also when the aggregation process is mechanically driven, as in the case of the formation of LB films.[2]

1.M. Caruso, E. Gatto, E. Placidi, G. Ballano, F. Formaggio, C. Toniolo, D. Zanuy, C. Aleman, M. Venanzi, Soft Matter (2014), 10, 2508.
2.M. Venanzi, E. Gatto, F. Formaggio, C. Toniolo J. Pept. Sci. (2017), 23, 104.

Self-assembling hexapeptide-polymer conjugates to be used as drug carriers

Federica Novelli, Serena De Santis, Cesare Giordano, Valerio Viali, Mattia Titubante, Giancarlo Masci, Anita Scipioni

Department of Chemistry, Sapienza University of Rome, P.le A. Moro, 00185-Rome, Italy

email: *anita.scipioni@uniroma1.it*

Keywords: conjugated L,D-peptide-polymer; poly(ethylene glycol); self-assembly; nanoparticles; drug loading

Well-designed hybrid functional biomaterials based on peptide-polymer conjugates are able to self-assemble into nanostructures useful for drug delivery since they allow a careful tuning of their self-assembling properties at nanometer scale. [1]. Among the strategies developed for peptide engineering, those characterized by peptides with regularly alternating enantiomeric sequences are particularly attractive, since they are able to self-assemble in stacks directed and stabilized by hydrogen bonds [2]. When the peptide and polymer are suitably chosen in order to achieve the proper balance of hydrophobic/hydrophilic regions, these conjugates are able to self-assemble in water in stable core-shell morphology nanoparticles with greater resistance to phagocytosis and, consequently, with enhanced circulation half-life.
Herein, the self-assembling properties of the conjugates Cbz-(L-Ala-D-Val)$_3$-NH-(CH$_2$-CH$_2$-O)$_{45}$-CH$_3$ (Pep$_6$-PEG, Cbz = carbobenzyloxy) and CH$_3$-(O-CH$_2$-CH$_2$)$_{45}$-C$_2$H$_2$N$_3$-(D-Leu-L-Trp)$_3$-NH$_2$ (PEG-Pep$_6$Trp) are investigated. The amphiphilic conjugates are characterized by the same length of the peptide moiety and PEG molecular weight but different amino acid sequence. Pep$_6$-PEG was obtained by end-linking the linear hexapeptides Cbz-(L-Ala-D-Val)$_3$-OH, obtained by solid phase peptide synthesis, to an amine-end functionalized poly (ethylene glycol) chain whilst PEG-Pep$_6$Trp was prepared through a highly efficient solid-phase synthesis by Cu(I) catalyzed azide/alkyne Huisgen 1,3-dipolar cycloaddition (CuAAC "Click" conjugation). The self-assembling behaviour of both conjugates was assessed by NMR, CD and fluorescence spectroscopies, DLS, and SEM microscopy. According to previous results, spectroscopic evidence suggests that the self-assembly process is ruled by the hydrophobic interactions and hydrogen bond network of peptide moiety; in the case of PEG-Pep$_6$Trp self-assembly, NPs are further stabilized by stacking interactions among indole groups. SEM micrographs (Figures 1A and B), where peculiar donought morphologies are apparent, and DLS data indicate that the conjugates self-assemble in NPs with a vesicular structure. Based on such findings, a structural model (Figure 1C) of NPs is proposed where two hybrid molecules self-assemble in head-to head (Pep$_6$-PEG) or tail-to-tail (PEG-Pep$_6$Trp) association with the peptide moiety forming the hydrophobic core of the aggregates whilst PEG in the outer shell confers stability to the system. The ability of the NPs to act as efficient drug delivery systems was investigated using curcumin as a model of hydrophobic drugs to evaluate the drug loading (DL) and pharmacokinetics. In spite of the similar structure of the aggregates, a good DL of 9 wt% and a sustained drug release over 72 hours was shown only for PEG-Pep$_6$Trp NPs, proving the importance of the hydrophobic peptide sequence to tune the DL and releasing ability of such kind of drug carriers.

[1] I. W. Hamley, Biomacromolecules 15 (2014) 1543-59.
[2] P. De Santis, S. Morosetti, and R. Rizzo, Macromolecules 7 (1974) 52-58.
[3] P. Punzi, S. De Santis, C. Giordano, M. Diociaiuti, F. Novelli, G. Masci, and A. Scipioni Macromol. Chem. Phys. 216 (2015) 439-49.

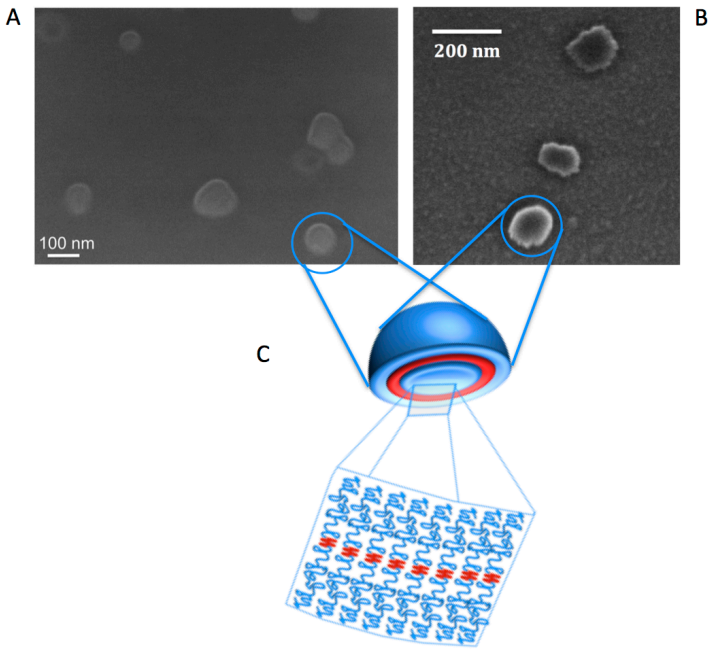

Figure 1 SEM micrographs of the hybrid conjugates Pep$_6$-PEG (A) and PEG-Pep$_6$Trp (B) with the peculiar donought morphologies; (C) Model of the vesicular structure of the aggregates obtained for self-assembly of Pep$_6$-PEG and PEG-Pep$_6$Trp in water.

Inclusion of antioxidants in mitochondriotropic core-shell drug delivery systems

Fabrizio Ciranna[a,b], Francesca Ceccacci[b], Simona Sennato[c], Michela Picano[d], Alessia Ciogli[e], Viviana Moresi[f], Eva Pigna[f], Giuseppina Bozzuto[g], Cecilia Bombelli[b]

[a]Consorzio Interuniversitario Reattività Chimica e Catalisi c/o Chemistry Department, Sapienza University, P.le A. Moro 5, Roma Italy
[b]CNR-IMC-Sezione Meccanismi di Reazione UOS Roma c/o Chemistry Department, Sapienza University, P.le A. Moro 5, Roma Italy
[c]CNR-ISC- UOS Sapienza c/o Physics Department, Sapienza University, P.le A. Moro 5, Roma Italy
[d]Sapienza University, Chemistry Department, P.le A. Moro 5, Roma Italy
[e]Sapienza University, Department of Chemistry and Technology of Drug, P.le A. Moro 5, Roma, Italy
[f]Sapienza University, Department of Anatomy, Histology, Forensic Medicine and Orthopedics Via Scarpa 14, Roma, Italy
[g]Centro Nazionale per la Ricerca e la Valutazione Preclinica e Clinica dei Farmaci, Istituto Superiore di Sanità, Viale Regina Elena 299, 00161 Roma, Italy
e-mail: cecilia.bombelli@uniroma1.it

Keywords: oxidative stress, cationic liposomes, remote loading, polymer coating

Mitochondria are the main source of reactive oxygen species (ROS) in the cells; for this reason they are equipped with natural defence systems (superoxide dismutase and several peroxidases) that, neutralizing ROS, prevent the oxidative damage to mitochondrial biomolecules. Nevertheless, under age-related dysfunctions or many pathological conditions, ROS level becomes too high, leading to severe damages to the organelle and, due to the key role of mitochondrion in the life of cells, to the whole organism. This is why the prevention of mitochondrial oxidative damage may be an effective therapeutic approach for many human degenerative diseases. This prevention can be achieved by different strategies, all hampered by the difficulty of delivering bioactive molecules to mitochondria. This difficulty is related to i) crossing of cell membrane ii) crossing the two membranes of the mitochondrion, the second of which being highly convoluted, densely packed, and displaying a strong negative potential. Therefore, mitochondrial delivery of drugs is a key issue for the treatment of several diseases related to oxidative stress, and, consequently, it is also an important topic in drug delivery system (DDS) development for subcellular targeting. With the final goal of delivering resveratrol and trolox, (Figure 1-2) two well-known antioxidants (AO), we developed a mitochondriotropic liposome-based DDS with a core-shell structure, (Figure 4) composed of

i) mixed liposomes, formulated with a natural phospholipid (1,2-dioleoyl-sn-glycero-3-phosphocholine, DOPC, or 1,2-dipalmitoyl-sn-glycero-3-phosphocholine, DPPC), the cationic triarilphosphonium bolaamphiphile **1** (Figure 3) and cholesterol, if need be. Because of the extended delocalization of the positive charge on the headgroups, **1** should favour the crossing of the mitochondrial membranes [1] guided by the negative potential of the inner membrane;
ii) a biocompatible polymer coating (BC), decorating the liposome. The BC, composed of polymers such as chitosan and dextran, is able to tune the surface properties, as charge, hydrophilicity and, more interestingly, it opens the possibility to specific functionalize liposome surface with proper moieties for the targeting of specific cells. Such a coating is also supposed to help liposomes to reach undamaged the cytosol and, finally, mitochondria.

Two different protocols, *i.e* passive loading in the lipid bilayer and active loading in the internal aqueous phase by the acetate gradient method, [2] were explored to load the antioxidant into liposomes. The entrapment efficiency (EE) of the antioxidants was determined by HPLC (resveratrol) or UV spectroscopy methods. Resveratrol and Trolox were loaded with very good AO/lipid ratio in cationic liposomes formulated with the mithocondriotropic bolamphiphile **1**. The active loading exploiting the calcium acetate gradient is very efficient also in the presence of bola **1**.
Laser scanning confocal microscopy (LSCM) investigations were carried out to assess the uptake and intracellular distribution of mithocondriotropic liposomes formulated with bola **1** in a murine skeletal muscle cell line (C2C12).
The coating process was developed by adding small aliquotes of the polymer to a liposome (or liposome-dextran) suspension and following the changes in Z potential and in particles diameter by DLS. The best conditions for coating liposomes with two layers of commercial dextran and chitosan by the *layer by layer* technique were assessed.

[1] V.Weisseig, V.P. Torchilin Advanced drug delivery reviews, 49 (2001) 127-149.
[2] S. Clerc, Y. Barenholz, Biochim. Biophys. Acta, 1240 (1995) 257-265.

Acknowledgments: CB, FC, SS are grateful for the financial support from FIRB2012 RBFR12BUMH. SS acknowledges support from PRIN 2012 SMART.

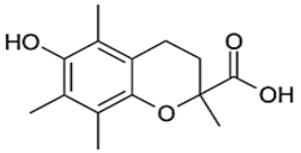

Figure 1. Chemical structure of the antioxidant Trolox

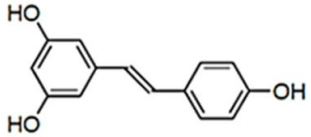

Figure 2. Chemical structure of the antioxidant *trans*-Resveratrol

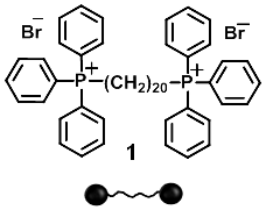

Figure 3. Chemical structure of the bolaamphiphile **1**.

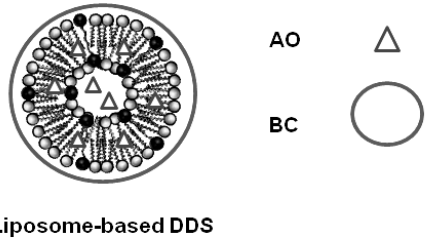

Figure 4. Representation of the liposome-based drug delivery system

Protein corona affects cellular uptake and intracellular trafficking of lipid nanoparticles

Luca Digiacomo[a,b], Daniela Pozzi,[a] Sara Palchetti,[a] Michelle A. Digman, Enrico Gratton[d], Francesco Cardarelli[c], Giulio Caracciolo[a]

[a] Department of Molecular Medicine, "Sapienza" University of Rome, Viale Regina Elena 291, 00161 Rome, Italy
[b] Department of Bioscience and Biotechnology, University of Camerino, Via Gentile III da Varano, 62032 Camerino, (MC), Italy
[c] Institute 3, City, Postal code, Country
[d] Laboratory for Fluorescence Dynamics, Biomedical Engineering Department, University of California, Irvine, Irvine, CA 92697, USA

e-mail: *giulio.caracciolo@uniroma1.it*

Keywords: (protein corona, lipid nanoparticles, intracellular trafficking, image correlation spectroscopy.)

Due to their intrinsic chemical-physical properties, lipid nanoparticles (NPs) are increasingly being employed as nanocarriers of therapeutic agents. Indeed, their high cytocompatibility, ease of functionalization and peculiar structure of closed bilayer vesicle, make them the most promising class of organic NPs for the treatment of many diseases.[1] Despite the advances in biomedical applications of NPs and numerous publications, few NPs have made it to clinical trials and even fewer have reached clinical practice.[2] This wide gap between bench discoveries and clinical applications is mainly because of our limited understanding of the biological identity of NPs. Under *in vivo* conditions lipid NPs get covered by an outer protein layer, which is formed when they come in contact with biological media (e.g. blood or plasma) and is commonly referred to as protein corona (PC).[3,4] To precisely predict the biological response to NPs, a deeper understanding of their in vivo biological identity (i.e., the PC structure) is needed. Thus, the PC is emerging as the 'game-changer' for the clinical application of NPs. However, so far it is not clearly understood how the PC impacts at cellular and sub-cellular levels and this is a crucial aspect for *in vivo* applications of biomaterials, especially for drug and gene delivery. To tackle this issue, we explored cellular uptake and intracellular dynamics of multicomponent lipid NPs in HeLa cells, by means of confocal fluorescence microscopy. Cellular uptake of lipid NPs was investigated by colocalization of fluorescence signals arising from lipid NPs and endocytic vesicles (Figure 1, panels A-C). According to previous findings, we focused on macropinocytosis, clathrin- and caveolin-mediated endocytosis (CME). Colocalization analysis of confocal images (Figure 1, panels D-F) showed that lipid NPs are mainly internalized by macropinosomes, while in presence of the PC clathrin-mediated endocytosis is the principal internalization pathway. Intracellular dynamics of lipid NPs was investigated by fluorescence correlation spectroscopy (FCS). In detail, we employed a fluorescence-based spatiotemporal fluctuation analysis method that makes possible to detect the mode of motion of vesicles from imaging, in the form of a mean square displacement (MSD) versus time-delay plot (image-derived MSD, hereafter referred to as *i*MSD).[5,6] The intracellular dynamics of lipid NPs and NP-PC complexes was compared to those of clathrin-coated endocytic vesicles, caveolae and micropinosomes. As Figure 2 clearly shows, the dynamical behaviour of lipid NPs closely resembled that of micropinosomes. On the other hand, dynamics of NP-PC complexes was more similar to that of clathrin-coated endocytic vesicles. By coupling results from colocalization studies and intracellular dynamics experiments, we claim that the PC is responsible for a switch in the internalization processes of lipid NPs, which, in turn, affects their intracellular trafficking mechanism.
These effects could be particularly relevant for a clinical use of NP-based delivery systems, whose cellular uptake and intracellular mode of motion determine their biological outcome. We predict that precise understanding of the role of NP-PC will yield fundamental insights and novel opportunities for accelerating the clinical translation of NPs from bench to bedside.

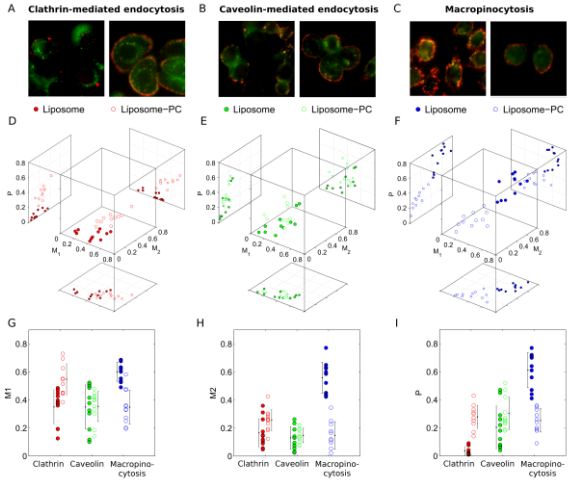

Figure 1: Colocalization images of red-labelled lipid NPs with with green-labelled endocytic vesicles, for (A) clathrin-mediated endocytosis, (B) caveolin-mediated endocytosis and (C) macropinocytosis. Results are expressed in terms of Manders coeffients (M1, M2) and Pearson's correlation coefficient, separately for each of uptake processes (D, E, F, respectively). (G, H, I) Projections of the measured values along the coordinate axes. Circles and circumferences correspond to liposome and liposome-PC complexes, respectively.

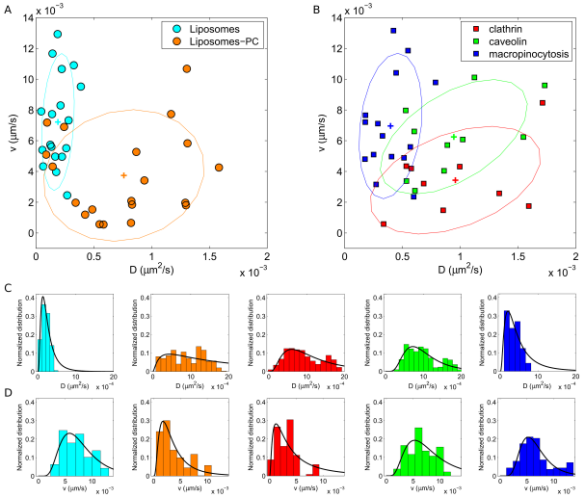

Figure 2: Dynamic parameters of (A) liposomes, liposome-PC complexes and (B) endocytic vesicles. Projections along the coordinate axes to obtain the corresponding distributions of (C) diffusion coefficients and (D) speed of the investigated objects. Distributions are weighted on the number of spots acquired in each time-series and take into account the experimental errors arising from the iMSD processing.

References:
[1] G. Caracciolo. Nanomedicine: Nanotechnology, Biology and Medicine (2015). 11(3) 543-577
[2] G. Caracciolo, O. C. Farokhzad, M. Mahmoudi. Trends in Biotechnology, (2017) 35 (3), 257-264.
[3] S.R. Saptarshi, A. Duschl, A.L. Lopata. Journal of Nanobiotechnology (2013). 11 (1).
[4] A. Salvati, A.S. Pitek, M.P. Monopoli, K. Prapainop, F.B. Bombelli, D. Hristov, P.M. Kelly, C. Aberg, E. Mahon, K.A. Dawson. Nature Nanotechnology (2013). 8, 137–143.
[5] C. Di Rienzo, E. Gratton, F. Beltram, F. Cardarelli. Proceedings of the National Academy of Sciences 110.30 (2013): 12307-12312.
[6] L. Digiacomo, M.A. Digman, E. Gratton, G. Caracciolo. Acta Biomaterialia (2016). 42, 189-198.

image Mean Square Displacement: a powerful tool for the characterization of intracellular dynamics of nanoparticles

Luca Digiacomo[a,b], Michelle A. Digman[c] Enrico Gratton[c], Giulio Caracciolo[a]

[a] Department of Molecular Medicine, "Sapienza" University of Rome, Viale Regina Elena 291, 00161 Rome, Italy
[b] Department of Bioscience and Biotechnology, University of Camerino, Via Gentile III da Varano, 62032 Camerino, (MC), Italy
[c] Laboratory for Fluorescence Dynamics, Biomedical Engineering Department, University of California, Irvine, Irvine, CA 92697, USA

e-mail: *giulio.caracciolo@uniroma1.it*

Keywords: (intracellular trafficking, nanoparticles, image correlation spectroscopy)

At a cellular level, the interactions among living matter and nanoparticle-based drug delivery systems highly regulate their dynamics and strongly affect their therapeutic efficiency.[1] Thus, manifold fluorescence techniques (including Single Particle Tracking (SPT) and Image Correlation Spectroscopy (ICS)) are increasingly being employed to study intracellular motions of fluorescence-labelled objects with high spatial and temporal resolution. However, none of these experimental tools has been specifically developed to take into account a spatial distribution of directed motions, commonly arising from the active transport of the labelled particles along cytoskeletal networks. To fulfil this gap, here we show how to characterize two-dimensional dynamics driven by Brownian diffusion and flow terms that are uniformly distributed in an angular range. Overall information about the investigated dynamics is obtained by decoupling the flow contributions, to quantify both the net displacement of the ensemble and the strength of the driving speed. These interdependent terms are related to the intrinsic anisotropy of the particle flow and its eventual symmetry, which arises when an angular dispersion affects the directionality of motion. The proposed approach exploits general concepts of the spatiotemporal image correlation analysis,[2] extends the image-derived mean square displacement method[3] and recovers dynamic and geometric features, which are commonly achieved through single particle analyses. In detail, starting from a time series of the collected fluorescence images, a spatiotemporal correlation function is computed and studied over the entire domain of the lag-variables (Fig. 1). Numeric simulations and in vitro experiments (Fig. 2) validated the method and demonstrate high stability in the measurement procedure, accurate description of the particle dynamics and low sensitivity to background. Furthermore, this procedure does not require the extraction of single particle tracks neither threshold-based criterions for the characterization of motion and provides a rapid measurement of the ensemble behaviour. Finally, despite this work focuses on directed motions and Brownian diffusions, we point out that the capabilities of the original approach[3] are preserved, thus confined motions and anomalous diffusions can be detected and the corresponding dynamic parameters can be measured. Therefore, we argue that this study will contribute to advance our understanding about the movement of nanoparticles in cells, their interactions with the biological environment and the subsequent effects on their therapeutic efficiency.

References:
[1] F. Cardarelli, L. Digiacomo, C. Marchini, A. Amici, F. Salomone, G. Fiume, A. Rossetta, E. Gratton, D. Pozzi, G. Caracciolo. Scientific Reports (2016). 6.
[2] B. Hebert, S. Costantino, P.W. Wiseman. Biophysical journal (2005). 88(5).
[3] C. Di Rienzo, V. Piazza, E. Gratton, F. Beltram, F. Cardarelli. Nature Communications (2014). 5.

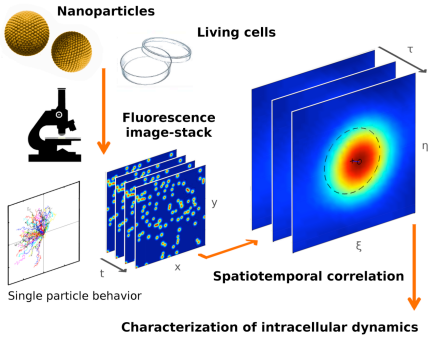

Figure 1. General scheme of an image correlation analysis: a fluorescence image time series is acquired and processed to get the autocorrelation function, which gives information about the investigated dynamics.

Microfluidic Manufacture of Cationic Lipid/DNA complexes

Luca Digiacomo[a,b], Sara Palchetti[a], Daniela Pozzi[a], Giulio Caracciolo[a]

[a] Department of Molecular Medicine, Sapienza University of Rome, Viale Regina Elena 291, 00161 Rome, Italy
[b] Department of Bioscience and Biotechnology, University of Camerino, Via Gentile III da Varano, 62032 Camerino (MC), Italy

e-mail: giulio.caracciolo@uniroma1.it

Keywords: nanomedicine, lipids, microfluidics, self-assembling, transfection efficiency

Recent advances in biotechnology have been achieved through the employment of microfluidic devices, both for the development of diagnostic tools and the preparation of nanomedicines. In this regards, the microfluidic mixing of therapeutic agents with biomaterials yields remarkably small systems, which can be designed for drug and gene delivery. Here we compared the ability of lipid vectors made of the same lipid species but prepared by means of two different techniques, to transfect Chinese Hamster Ovarian (CHO) cells. The techniques employed are: microfluidic mixing of the components[1] and self-assembling process. In detail, we measured the transfection efficiency (TE) as the detected luciferase signal per mass unit of cell proteins, at different lipid-to-DNA mass ratios. Results are expressed in terms of luciferase signal l, amount of cellular proteins p and DNA concentration c, for each of the investigated samples. Fig. 1A shows the measured transfection efficiency, as l/p at different c-values. For complexes prepared both by self-assembling and microfluidic mixing, linear trends can be recognized and quantified by fitting the experimental data. Furthermore, similar patterns are exhibited by the absolute luminescence l (Fig 1B), which represents the total detected signal, without any information about the number of living cells in the sample. Hence, if l=p and l vary linearly with c, their trends can be described as follows:

$$\begin{aligned} l/p &= A_0 + A_1 c \\ l &= B_0 + B_1 c \end{aligned} \qquad (1)$$

where the coefficients A_0, A_1, B_0 and B_1 depend on the preparation technique. In other words, both the luminescence signal per cell and the total luminescence increase with the DNA amount administrated to cells. Despite this represents a reasonably predictable outcome, the relationships expressed in Eq. 1 describe coupled variables and thus can be easily managed to obtain the expected behavior of the cellular protein amount, as a function of c, which reads

$$p = (B_0 + B_1 c)/(A_0 + A_1 c) \qquad (2)$$

Therefore, p(c) describes a hyperbola, with intercept $p_0=B_0/A_0$ and horizontal asymptote $p_1=B_1/A_1$. In this regard, Fig. 1C shows experimental data and corresponding fitting curves.
Although for both self-assembling and microfluidic mixing the experimental data follow the aforementioned relationships, each procedure has its specific trends. As an instance, both l/p and l are higher for the former technique, thus suggesting that at any DNA concentration those systems transfect more than those prepared by microfluidic mixing (Fig. 1A, 1B). The measured control values are (1.26±0.6) 10^2 RLU/μg and (1.20±0.5) 10^3 RLU respectively, i.e. at least three orders of magnitude lower than the curves. From this perspective, we can infer that both the techniques provide effective systems for transfection experiments and the self-assembling procedure has slightly superior performances than the microfluidic mixing. However, this scheme is inverted for the curves describing the amount of cellular proteins (Fig. 1C). Indeed, the decreasing trend of p(c) is much more steeper for complexes prepared through self assembling, which induces a remarkable fall of the p-values at high DNA concentrations. This represents a noteworthy result, since the detected amount of cellular proteins is strictly related to the number of living cells in the sample and thus it gives information about the cytocompatibility of the complexes.[2] This relationship between "therapeutic" effect and side effect of the complexes can be viewed also in a representation of the involved variables, decoupled and plotted in a (l; p)-parameter space (Fig. 1D). Furthermore, we point out that the measured transfection efficiencies are comparable with those of other lipid formulations on the same cell line and slightly lower than that of Lipofectamine, a gold standard of the transfection reagents. Thus, the most notable difference between self-assembling and microfluidic mixing relies on the cytocompatibility of the resulting systems.

[1] J. A. Kulkarni et al., Nanomedicine: Nanotechnology, Biology and Medicine 75 (2016) 191-197.
[2] M. Rasoulianboroujeni et al., Materials Science and Engineering: C 13 (2016) 1377–1387.

.

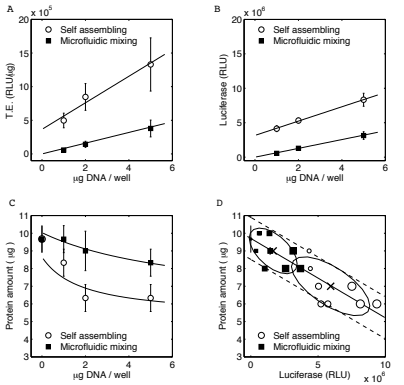

Figure 1. Transfection Efficiency (TE) of lipoplexes and DNA-lipid NPs, synthesized by self-assembling and microfluidic mixing, respectively. (A) Luciferase signal per protein amount as a function of the DNA concentration, (B) total detected luminescence signal and (C) measured amount of proteins. The lines show fitting curves of the results. (D) Resulting scatter plot of the aforementioned variables. The lines indicate a linear regression trend (within experimental errors), larger marker sizes correspond to higher DNA concentrations, ellipses are centered at the average values (”X”) of the distributions and are evaluated by diagonalizing the corresponding covariance matrices.

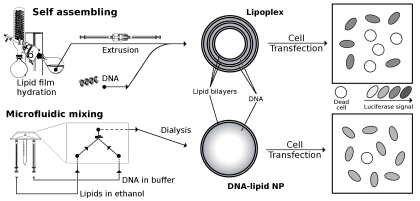

Figure 2. Representative scheme of the main outcomes. Liposomes are synthesized by lipid film hydration, then extruded and mixed with DNA to obtain lipoplexes. Conversely, DNA-lipid NPs are prepared by microfluidic mixing of the components, followed by an overnight dialysis. The transfection efficiency of lipoplexes is slight higher than DNA-lipid NPs, however the latter complexes are remarkably more cytocompatible.

Detection of tumours biomarker enzymes by using polydiacetylenic liposomes

Sara Battista [a], Barbara Altieri [a], Giorgio Cerichelli [a], Luisa Giansanti [a, b].

[a] Department of Physical and Chemical Science, University of L'Aquila, Coppito (AQ), 67100, Italy
[b] CNR-Istituto di Metodologie Chimiche, Monterotondo Scalo (RM), 00016, Italy

e-mail: sara.battista@graduate.univaq.it

Keywords: liposomes, sensor, biomarker, 5-fluorouracil, polydiacetylene

5-Fluorouracil (5-FU) is a strong chemotherapeutic drug, widely employed in the treatment of some of the most frequently solid tumours (breast, colon, and skin cancer[1]). Thymidylate synthase, thymidine phosphorylase (TP) and dihydropyrimidine dehydrogenase are the three target enzymes of 5-FU and take part to the metabolism of pyrimidines. Their presence or their absence in biological fluids is indeed related to a specific state of health because 5-FU has a very narrow therapeutic window[2]. Based on these premises, there is the need of a fast, precise and cheap method for dosing the activity of these enzymes before and during 5-FU treatment to reduce its sever side effects and increase its efficacy.
Polydiacetylene (PDA)-based materials are largely investigated for their sensing potentialities because the *ene-yne* moiety confers them peculiar optical properties and make them sensitive to external stimuli[3]. The ability of different specific PDA liposomes to give an optical response upon the interaction with TP, one of the target enzymes of 5-FU, was investigated. Liposomal formulations contain 10,12-pentacosadiynoic acid in the presence or in the absence of 1,2-dioleoyl-*sn*-glycero-3-phosphocholine or 1,2-dimirystoyl-*sn*-glycero-3-phosphocholine. To make them specific for TP, one of the three non-ionic surfactants **1**, **2** and **3** in which polyoxyethylene spacers of different length (Figure 1) link a 5-FU molecule to a diacetylenic hydrophobic chain. These formulation polymerize upon irradiation and, thanks to the presence of 5-FU, can show a colorimetric variation upon the specific interaction with TP.

[1] J. L. Arias, Molecules 13(2008) 2340.
[2] P. Alvarez, J.A. Marchal, H. Boulaiz, Expert Opin. Ther. Patents 22(2) (2012) 107-123.
[3] J. Lee, H. Jun, J. Kim, Adv. Mater. 21(2009) 3674.

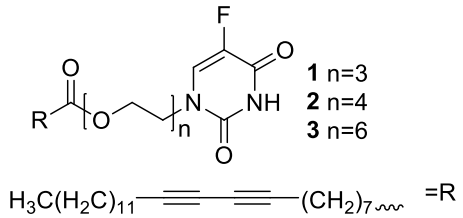

Figure 1. Molecular structure of non-ionic diacetylenic surfactant **1, 2** and **3**.

In vitro biocompatibility study of sub-5 nm silica-coated magnetic iron oxide fluorescent nanoparticles for potential biomedical application

Mario Ledda [a], Daniela Fioretti [a], Sabrina Foglia [b], Massimiliano Papi [c], Giovanna Iucci [d], Giovanni Capellini [d], Maria Grazia Lolli [a], Settimio Grimaldi [a], Monica Rinaldi [a#] and Antonella Lisi [a#]

[a] Institute of Translational Pharmacology (IFT), Department of Biomedical Sciences, National Research Council (CNR), Rome, 00133, Italy

[b] Institute of Materials for Electronics and Magnetism (IMEM), Department of Engineering, ICT and technologies for energy and transportation, National Research Council (CNR), Parma, 43124, Italy

[c] Institute of Physics, Catholic University of the Sacred Heart, Rome, 00168, Italy

[d] Department of Science, University Roma Tre, Rome, 00146, Italy

[#]These authors shared senior authorship

e-mail: Antonella.lisi@ift.cnr.it

Keywords: ultra-small Fe_3O_4 nanoparticles; superparamagnetic; functionalization; nanomedicine

Nanoparticles (NPs) made up of components between 1 nm and 100 nm in size and specifically magnetic iron oxide nanoparticles (IONPs), approved by Food and Drug Administration (FDA) [1], have been extensively studied and have attracted much interest for their intriguing properties employable in a wide range of biomedical applications (Figure 1).

NPs are used for diagnosis, prevention and treatment of diseases as much as for tissue engineering and regenerative medicine applications. These implementations demand the cross communication among different disciplines for the success of new therapies in restoring and regenerating the normal function of damaged cells, organs and tissues.

The scientific rationale for the present multidisciplinary study is suggested by the need to design innovative and safe strategies to deal with human diseases.

We synthetized and characterized ultrafine 3 nm superparamagnetic water-dispersible nanoparticles, prepared by an "arrested precipitation strategy". By a facile and inexpensive one-pot approach, nanoparticles were coated with silica to prevent their degradation/aggregation and to increase their surface functionalization, and contemporarily labelled with fluorescein isothiocyanate (FITC) dye to visualize their intracellular localization.

The resulting new sub-5 nm silica-coated magnetic iron oxide fluorescent (sub-5 SIO-Fl) nanoparticles were tested in CaCo-2 cell line, a well characterized model of the intestinal epithelium, commonly used for biopharmaceutical evaluations as well in toxicity studies either as differentiated or undifferentiated cells [2].

We studied sub-5 SIO-Fl nanoparticles cellular uptake and intracellular localization. Furthermore, we investigated if their uptake affected CaCo-2 cell morphology, growth, viability, cell cycle distribution, as well as transcriptional, translational and secretory activities, in a dose-dependent manner. To further shed light on their biocompatibility, the effect of the sub-5 SIO-Fl nanoparticles on CaCo-2 cell differentiation and pro-inflammatory response was analysed.

Overall, these results showed the in vitro biocompatibility of the sub-5 SIO-Fl nanoparticles promising their safe employ for diagnostic and therapeutic biomedical applications.

Since their magnetic nature, our nanoparticles could be easily in vivo directed toward the desired tissues/organs to shuttle drugs upon the application of an external static magnetic field. They could be used as efficient vehicles for drug/gene delivery for antiblastic therapies, enhancing the efficacy of treatments with reduced systemic toxicity. Moreover, these nanoparticles can maintain the ability to act as antennae in an external alternating magnetic field to convert electromagnetic energy into heat, to synergize the action of the shuttled drugs with hyperthermia [3].

[1] A. L. Cortajarena *et al.*, Nanobiomedicine 1 (2014) 1-20.
[2] K. Gerloff *et al.*, Nanotoxicology 7 (2013) 353-366
[3] T. Kobayashi, Biotechnol. J. 6 (2011)1342-1347.

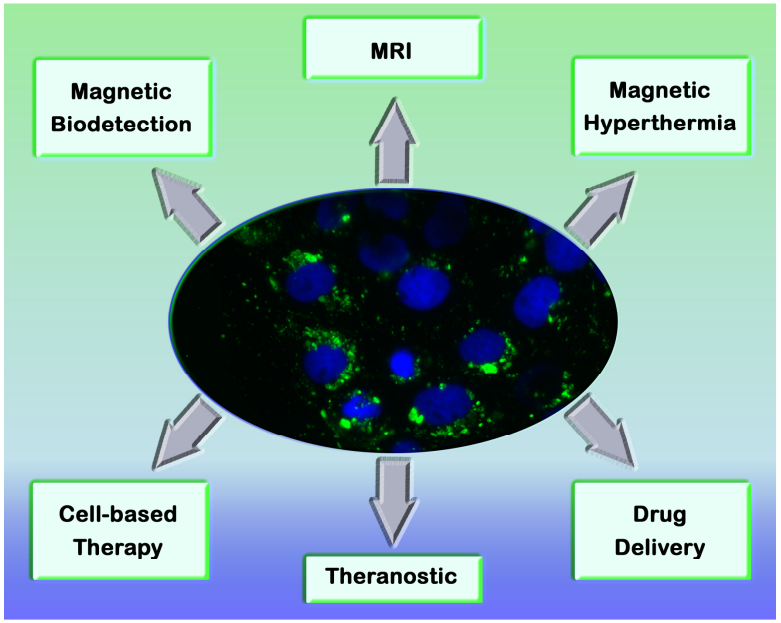

Figure 1. Magnetic nanoparticles cellular internalization and biomedical applications.

Ethanol sensor based on self-assembled polystyrene photonic crystal

L. Burratti [a], M. Casalboni [a], F. De Matteis [a], R. Pizzoferrato [b], I. Cacciotti [c], P. Prosposito [a]

[a] Industrial Engineering Department, INSTM and CIMER, University of Rome Tor Vergata, Via del Politecnico, 1 00133 Rome, Italy
[b] Industrial Engineering Department, University of Rome Tor Vergata, Via del Politecnico, 1 00133 Rome, Italy
[c] Engineering Department, INSTM RU, University of Rome Niccolò Cusano, via Don Carlo Gnocchi, 3 00166 Rome, Italy
e-mail: paolo.prosposito@uniroma2.it

Keywords: (Photonic crystals, VOC, alcohol sensors)

Volatile organic compounds (VOCs), which have high vapor pressure at room temperature [1], are dangerous contaminants in the work and home environments. Alcohols are a class of VOCs, of which the most common are methanol, ethanol, 1-propanol, isopropanol and n-butanol. It is extremely important for human safety and health to be able to detect the presence of these contaminants at low concentrations. Recently, sensors based on Photonic Crystals (PCs) able to detect VOCs presence were presented [1,2]. PCs are periodic dielectric structures, which are characterized by a refractive index (RI) modulation. Opals are the simplest 3D-PCs, they are formed by dielectric spheres organized in a face centered cubic (*fcc)* lattice [3]. The diffraction of light by PCs is described by a combination of Bragg and Snell's laws [3]. In general, the working principle of these types of optical sensors is based on a variation of n_{eff} (effective refractive index) [4] and a consequent shift of the diffraction peak, since the n_{eff} of the PC depends on all the dielectric materials forming the devices (spheres and voids).

We fabricated very good quality opal films of polystyrene (PS) monodispersed spheres by *drop-casting* on pre-treated glass substrates. Figure 1 reports SEM micrograph of a polystyrene PC. We tested the samples as alcohol vapor detectors with methanol, ethanol, 1-propanol, isopropanol and n-butanol. In particular, we studied the time-dependence of the reflectance peak of the PCs in the presence of the different alcohols. In the presence of saturated vapor alcohols, the PC porosity is filled by the vapor and a subsequent condensation inside the pores determines an enhancement of the effective refractive index and a subsequent redshift of the diffraction peak. When all the pore volumes are completely saturated, the reflectance-peak wavelength reaches a plateau value and the response of the PC can be considered as complete. Moreover, to justify the strong effect observed on the redshift, a second process has to be taken into account, namely a small swelling of PS particles induced by the alcohols. A different mechanism is valid for water since it shows a very small redshift. The surface nanostructuring (due to the nanospheres) makes the entire PC hydrophobic, thus avoiding the infiltration of the condensed water inside the porous structure. This effect is connected with the high polarity of the water. Responses (peak wavelength redshifts) of the PCs to different VOCs are presented in figure 2. The different behaviors of water and ethanol suggested that we investigate the possible use of PCs as a breathalyzer to test the content of ethyl alcohol. To modify the concentration of ethanol, we changed the relative volumes of water and ethanol in the sample chamber. Two regions can be identified. The first one, at high ethanol concentrations (> 80 % V_{EtOH}/V_{Sol}), where the presence of the alcohol is so high to saturate completely the voids between PC nanoparticles. In this range, the response is always maximum. The second region (below 70 % V_{EtOH}/V_{Sol}) is characterized by a linear behavior, here the condensation of ethanol is still valid, but its amount is not enough to completely fill the voids of the PCs, but it can fill them only partially and proportionally to its concentration. The estimated detection limit of ethanol for our sensor is of 2%.

[1] Wang, Fengyan, et al. "Cellulose photonic crystal film sensor for alcohols." Sensors and Actuators B: Chemical 220 (2015): 222-226.
[2] Kuo, Wen-Kai, et al. "A bioinspired color-changing polystyrene microarray as a rapid qualitative sensor for methanol and ethanol." Materials Chemistry and Physics 173 (2016): 285-290.
[3] Serpe, Michael J., Youngjong Kang, and Qiang Matthew Zhang, eds. *Photonic Materials for Sensing, Biosensing and Display Devices*. 2016.
[4] Schutzmann, S., et al. "High-energy angle resolved reflection spectroscopy on three-dimensional photonic crystals of self-organized polymeric nanospheres." *Optics express* 16.2 (2008): 897-907.

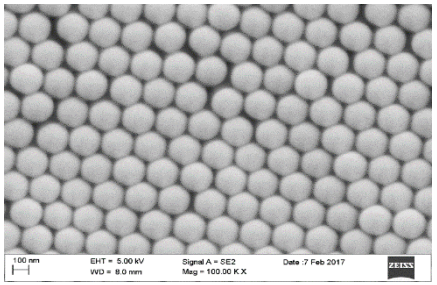

Figure 1. SEM micrograph of polystyrene PCs. sample.

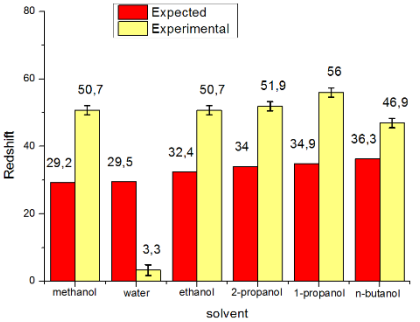

Figure 2. Comparison between theoretical calculation (red bars) and experimental data (yellow bars).

ElectroSpray Ionisation Deposition for biosensor application

J. Chiarinelli[a,c], M.C. Castrovilli[a] , N. Cicco[b], P. Bolognesi[a], P. Calandra[d] , D. Centonze[f] ,A. Cartoni[a,g], L. Avaldi[a]

[a] *CNR, Istituto di Struttura della Materia, Area della Ricerca di Roma 1, Monterotondo Scalo, Italy*
[b] *CNR, Istituto di Metodologie per l'Analisi Ambientale, Zona Industriale - Tito Scalo (PZ), Italy*
[c] *Dipartimento di Scienze, Università di RomaTre, Roma, Italy*
[d] *CNR, Istituto per lo Studio dei Materiali Nanostrutturati, Area della Ricerca di Roma 1, Monterotondo Scalo, Italy*
[f] *Dipartimento di Scienze Agrarie, degli Alimenti e dell'Ambiente, Università degli Studi di Foggia, Italy*
[g] *Dipartimento di Chimica, 'Sapienza' Università di Roma, Roma, Italy*

e-mail: jacopo.chiarinelli@ism.cnr.it; paola.bolognesi@cnr.it

The ElectroSpray Ionization (ESI) developed by Fenn et al. [1] allows to bring large organic molecules (proteins, enzymes etc) as intact and isolated units in the gas phase. The technique is based on the use of a low-concentration solution of the molecule of interest flowing in a small capillary held at high voltage (typically a few kV) with respect to a grounded counter electrode placed some 10-15 mm away. On the tip of the emitter, the surface tension of the liquid cannot support the formed charge and therefore the liquid forms the so-called 'Taylor cone' inside which a Coulomb explosion creates a spray of charged droplets. The size of the droplets continue decreasing as the solvent evaporates by releasing a gas of molecular ions. The ESI process usually takes place in the air (Figure 1a) and then the jet can be transported into a vacuum chamber for the analysis. Originally developed for protein studies with mass spectrometry, ESI was then used with other types of systems (polymers, Nanoparticles, bacteria ...) as well as for different applications, as 'soft-landing' deposition. In these cases, the apparatus combines electrostatic transport and filter devices, to select the ions of interest and guide them towards either a spectrometer for the analysis or a surface for the deposition.

Such a device is under construction at the CNR-ISM Montelibretti. Presently, it consists of i) a heated capillary to transport the charged species in vacuum and ii) a first differential pumping stage equipped with an octupole ion guide, see Figure 1b. A vacuum chamber housing a quadrupole mass spectrometer (QMS) for mass-over-charge, m/z, selection of the charged species, followed by a quadrupolar deflector to direct them towards a deposition chamber is being designed and will soon be commissioned. All in all, an in-vacuum 'soft-landing' deposition apparatus opens-up the unique possibility to perform m/z selected deposition in UHV condition of large biomolecular species [2], with control over the kinetic energy of the deposited species. On the other hand it is a quite complex and costly set-up, suffering severe limitations due to the low fluency of the m/z selected species. The main long term goal of the project is to increase the intensity of the ESI beam by mean of a customised, home-made, apparatus in order to make 'soft landing' a competitive technique for nanotechnology applications such as the production of biosensors and organic devices.

In parallel to the design of the in-vacuum apparatus, the potentiality of the ElectroSpray Ionisation technique for the deposition of active enzymes is being tested using a simpler set-up for 'in-air' deposition. This approach provides effective removal of the solvent, with the advantages that the deposition can be carried out at ambient pressure or in controlled atmosphere, with significant reduction of costs and times of the process, which could be easily automatized and applied on large scale.

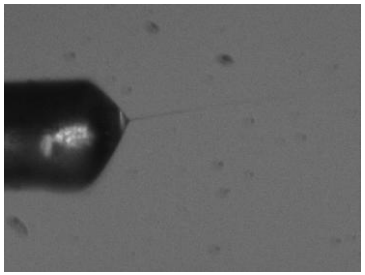

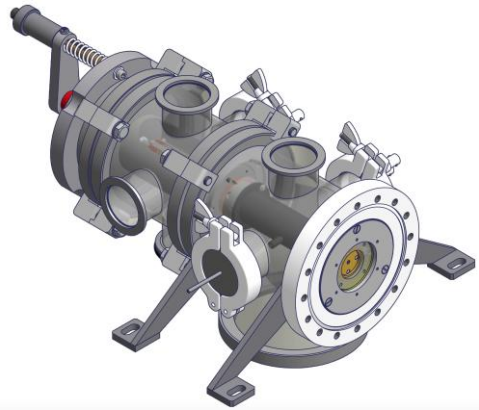

Figure 1a (top). The Taylor cone and ESI beam. The inner diameter of the needle is 0.1 mm.
Figure 1b (right). The non-commercial ESI source at the CNR-ISM, Montelibretti, made of a heated capillary and a octupole ion guide *[Design from Aarhus University]*.

Laccase, a well-known enzyme used for the detection of polyphenols in different matrices [3,4] is used for these studies. Various experimental conditions, such as needle sizes and voltages, flow rate, type and amount of solvents, pH solution, geometry of the ESI-support system, are being evaluated in order to assess the performances of the ESI technique for biosensor fabrication. The enzimatic activity of Laccase prior to deposition and after dissolution in buffer of the deposited material is verified and compared by using syringaldazine colorimetric essay [5].

Solvents play a crucial role both for the ESI process as for the preservation of enzyme activity. We observed that the presence of the ethanol or methanol solvents (20% concentration) does not affect the value of absorbance with respect to the Laccase in pure buffer solution (pH 5.5). Therefore, as a preliminary test, a concentration of 0.2 μg/μl of laccase in a solution of 80% water and 20% of ethanol or methanol (with or without the addition of 0.01 % of formic acid) has been used to deposit 6 μg of Laccase on conductive polymer (Polyethylene terephthalate, PET) substrates. The results of the spectrophotometric measurements with syringaldazine assay showed:

- negligible difference between ethanol/methanol solvents, at least at the chosen conditions, where the value of absorbance of the Laccase deposited and re-dissolved is 70% with respect to the one not undergone ESI deposition. The loss of 30% activity can be attributed to the overall effects of the ESI process and effectiveness in the extraction of the deposited material.
- negative effects due of the presence of the formic acid, even at 0.01 % concentration, with a residual value of absorbance of about 10%.

To investigate the immobilisation on screen printed electrodes (SPE) as well as the homogeneity of deposition at different scales, measurements with an Atomic Force Microscope (AFM) and a profilometer are also being performed.

Acknowledgment.
This work is partially supported by the Italian Ministry of Foreign Affairs and International Cooperation (MAECI) via the Serbia–Italy Joint Research Project "A nanoview of radiation-biomatter interaction"

References.

[1] J.B. Fenn et al., Science 4926 (1989) 64; The Nobel Prize for Chemistry 2002.
[2] D.E. Clemmer, R. R. Hudgins, M. F. Jarrold, J. Am. Chem. Soc. 117 (1995) 10141−10142.
[3] M.M. Rodríguez-Delgado et al. Trends in Analytical Chemistry 74 (2015) 21–45.
[4] M. Verrastro et al. Talanta 154 (2016) 438–445.
[5] J.P. Ride, Physiological Plant Pathology 16 (1980) 187-196.